EUMETSAT/ECMWF Fellowship Programme,
Research Report No. 15

Evaluation of calibration and potential for assimilation of SEVIRI radiance data from Meteosat-8

Matthew Szyndel, Graeme Kelly,
Jean-Noël Thépaut

September 2004

ECMWF
Shinfield Park
Reading
RG2 9AX
United Kingdom

For additional copes please contact: library@ecmwf.int

Series: EUMETSAT/ECMWF Fellowship Programme – Research Reports

A full list of ECMWF Publications can be found on our web site under:
http://www.ecmwf.int/publications/

© Copyright 2004

European Centre for Medium Range Weather Forecasts
Shinfield Park, Reading, RG2 9AX, England

Literary and scientific copyrights belong to ECMWF and are reserved in all countries. This publication is not to be reprinted or translated in whole or in part without the written permission of the Director. Appropriate non-commercial use will normally be granted under the condition that reference is made to ECMWF.

The information within this publication is given in good faith and considered to be true, but ECMWF accepts no liability for error, omission and for loss or damage arising from its use.

Abstract

Data from the SEVIRI instrument flown on the Meteosat-8 spacecraft are described. The characteristics of the data are compared to data from the nearest equivalent channels from HIRS instruments. Assimilation trials are described and the results of these trials presented and discussed.

1 Introduction

The first Meteosat Second Generation (MSG) spacecraft was declared operational and designated Meteosat-8 on 29th January, 2004. This spacecraft carries the Spinning Enhanced Visible and Infrared Imager (SEVIRI) as the successor to the Meteosat Visible and Infrared Imager (MVIRI) instrument carried by earlier Meteosat spacecraft. SEVIRI has 12 channels, 8 of which are in the infrared, compared to MVIRI's 3 channels (1 visible, 2 infrared). SEVIRI also has a higher spatial resolution and takes images more frequently. The instrument is described in Schmetz *et al.*.

EUMETSAT create a clear sky radiance (CSR) product for MSG. This product is generated by cloud classifying every pixel in an image and finding the average radiance for groups of 256 pixels (16 pixel by 16 pixel squares referred to as 'segments') summing over cloud free pixels. These data are provided with the cloud free fraction for each segment and a number of quality indicators (e.g. standard deviation of cloud free pixel radiances, confidence in cloud clearing). See Köpken *et al.* for details. This document discusses the quality of SEVIRI radiance data against the ECMWF Integrated Forecast System (IFS) and against HIRS observations. Tests of assimilation strategies for the MSG clear sky radiance product are then discussed.

2 Data Quality

Initial monitoring of CSR data for the water vapour channels of Meteosat-8 gave promising results. The $6.2\mu m$ channel showed an (O-B) bias of -1.7 K and an (O-B) standard deviation of between 1.5 K and 2.0 K varying through the assimilation window. The $7.3\mu m$ channel gave an (O-B) bias of 0.7 K and a standard deviation of (O-B) of between 1.2 and 1.6 K, again varying with time through the assimilation window. Both channels showed a diurnal cycle in first guess departure with a peak-to-peak amplitude of order 0.4 K – see figures1 and 2. A cycle with period 12 hours is evident in the standard deviation of first guess departure – this is due to the forecast length of background data growing through the assimilation window.

Scatter plots of the first guess departure of data against percentage clear showed that there is a slight correlation between the two values, with cloudier segments showing a slightly colder first guess departure in both the 6.2 μm and 7.3 μm channels – see figure 3. This correlation together with the above mentioned diurnal cycle in first guess departure may indicate problems with cloud clearing.

3 Cross Calibration

This section provides an intercomparison of HIRS radiances and Meteosat-8 SEVIRI radiances. The HIRS radiances are level-1c radiances from NOAA-16 and -17, cloud cleared by ECMWF, and restricted to the area north of 50°S, south of 50°N, east of 50°W and west of 50°E. The Meteosat-8 radiances are the EUMETSAT clear sky radiance product for the same area. The comparison is in fact made between the area mean observation minus ECMWF model first guess, referred to as first guess departure. Time series of these values with a 6 hour averaging window are compared. While at times the HIRS coverage of this area is not complete, smaller areas lead to more sampling noise in the time series. Comparisons are made for SEVIRI channels 4-11, with the

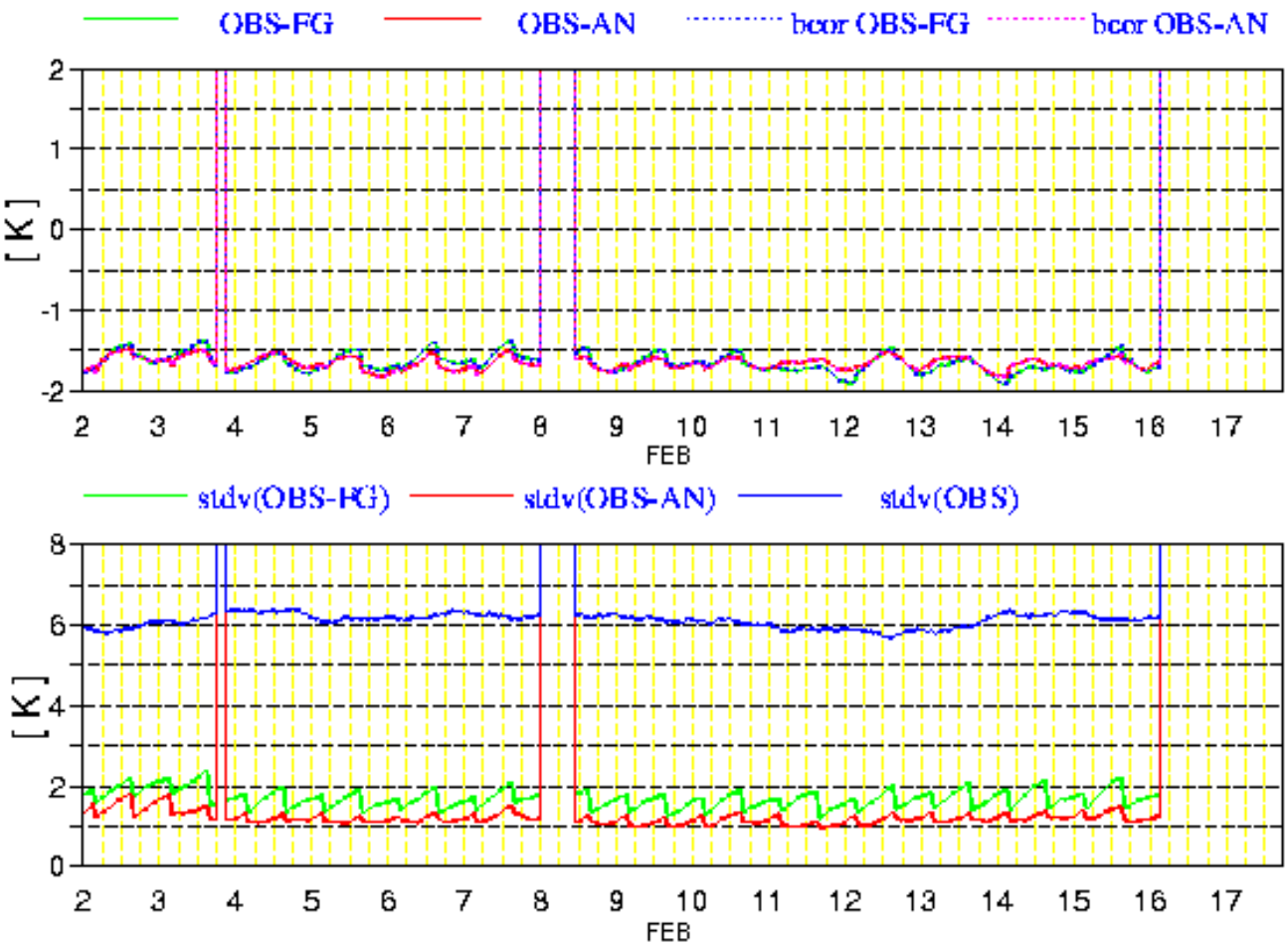

Figure 1: Top panel: Mean observation departures for Meteosat-8 6.2 μm channel summing over all data with cloud free fraction 0.7 or greater. Bottom panel: Standard deviation of observations and observation departures for Meteosat-8 6.2 μm channel summing over all data with cloud free fraction 0.7 or greater.

exception of channel 7 as HIRS/3 has no channel in the 8.7 μm region. Finally a comparison is made between simulated SEVIRI radiance data using two different formulations of RTTOV, the NWPSAF rapid radiative transfer model. Regression coefficients are used with the standard RTTOV formulation, where the spectral radiance is considered independent of wavelength across the spectral filter function of an instrument. A second set of coefficients is used where the radiance is assumed to follow a Planck function (Brunel and Saunders). For broad channels this should improve the modelling of radiances. For the WV channel on MVIRI this change in RTTOV reduces the bias between simulated and observed brightness temperatures by around 1 K.

3.1 Cloud clearing

3.1.1 SEVIRI

SEVIRI channels are cloud classified using a series of threshold and differencing tests as described in Lutz *et al.*. Cloud height is then estimated. All channels are considered cloudy if cloud is found at any level, with the exception of the 6.2 μm channel which is considered cloudy if cloud is found above 700 hPa.

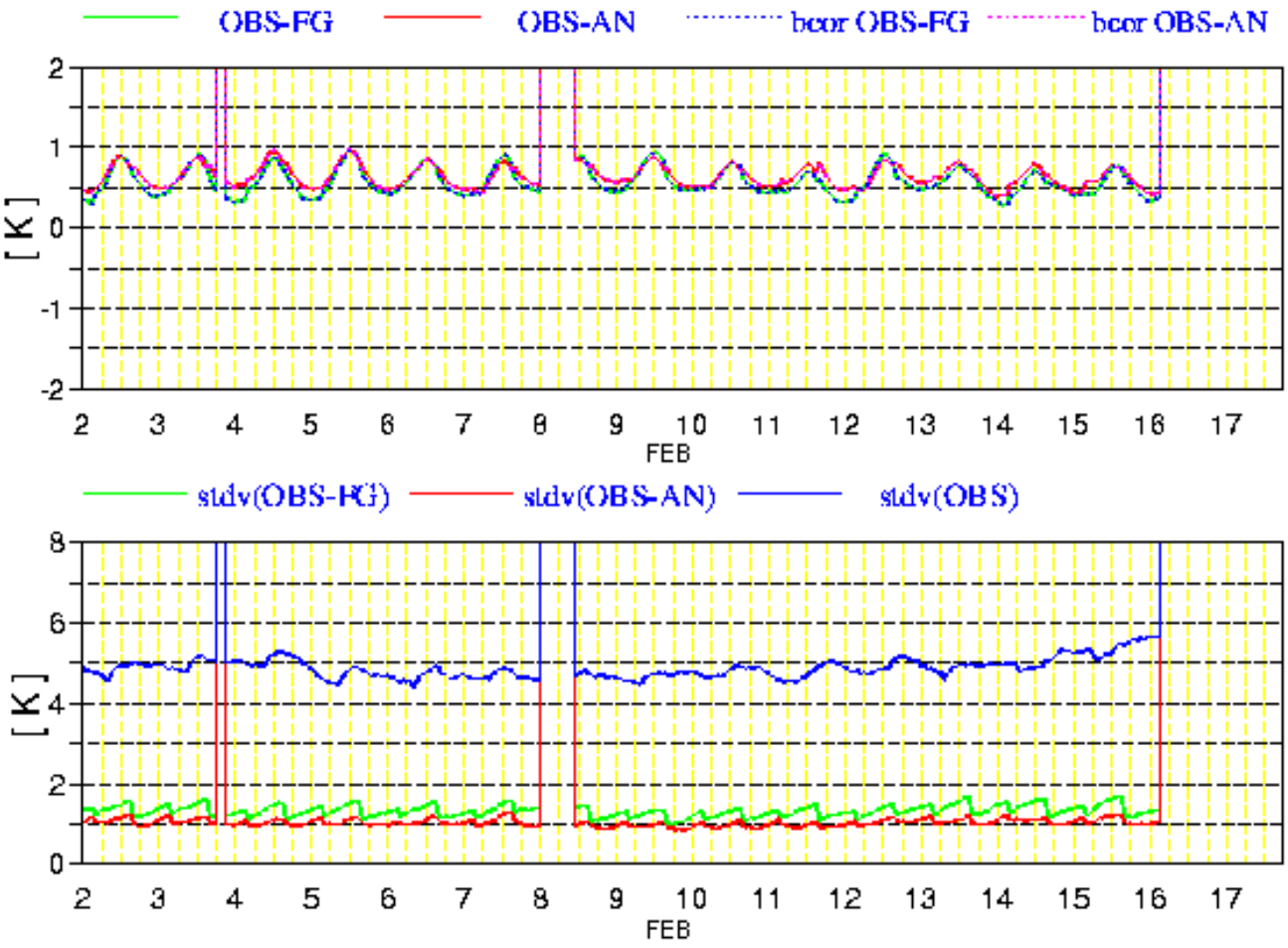

Figure 2: As figure 1 but for Meteosat-8 7.3 μm channel.

3.1.2 HIRS

HIRS channels are cloud cleared by ranking the longwave CO_2 channels (channels 2 to 7) in order of weighting function peak height. It is assumed that the highest channel used, channel 2, is cloud free. The first guess departure is calculated for these channels and normalised by the first guess departure standard deviation for each channel. The difference in these values for adjacent pairs of channels is calculated and compared to a critical value; if the value is exceeded the lower channel of the pair and all channels below it are considered cloudy. Shortwave CO_2 channels and water vapour channels are associated with a longwave channel with a weighting function at a similar height. A window channel check is performed to identify low cloud.

3.2 3.9 μm channel

The closest HIRS channel to the SEVIRI 3.9 μm channel is channel 18 – see figure 4. The SEVIRI channel is considerably broader, and consequently samples radiation in a region of strong CO_2 absorption at the longwave end of the spectral response function, making the SEVIRI channel more sensitive to upper air temperatures. A water vapour feature at the shortwave end of the SEVIRI response function may also give sensitivity to water vapour.

Figure 5 shows the time averaged monitoring statistics of the two channels with respect to the ECMWF integrated forecast system (IFS). The graph shows four points per day to give a smooth line for the HIRS instrument.

Unfortunately our radiative transfer model at present does not model reflected solar radiation, a major contributor to the observed radiances in these channels. Consequently the daytime first guess departures should be ignored. The nighttime values appear to lie between -0.8 K and -1.0 K for cloud cleared HIRS channel 18 radiances from NOAA-17. NOAA-16 measurements lie between -0.8 K and -1.2 K. For SEVIRI CSRs the departures lay at about -2.4 K using flat RTTOV coefficients; using Planck weighted coefficients the value is closer to -0.2 K. This large difference indicates significant problems for RTTOV simulation of this broad, short wavelength channel, which may go some way to explaining the discrepancy between the two channels. Furthermore the significant difference in the weighting functions of these channels arising from CO_2 and H_2O dependence in the SEVIRI channel makes direct comparison somewhat optimistic.

For all four measurements (2 HIRS and SEVIRI simulated two ways) the standard deviation of first guess departure at night appears to be around 1.0K.

3.3 Water vapour channels

HIRS channels 11 and 12 most closely resemble the SEVIRI water vapour channels. Spectral response functions are shown in figures 6 and 7. While the SEVIRI 6.2 micron channel is broader than HIRS channel 12 the region of the spectrum observed is all strongly interactive with water vapour and as a result the two channels should behave very similarly. The SEVIRI 7.3 μm channel is at the edge of the water vapour band and as a result will not match HIRS channel 11 as well as the 6.2 μm channel matches HIRS channel 12.

Figure 8 shows model first guess departures for the 6.2μm channel and HIRS channel 12. The NOAA-17 HIRS measurements have a -0.8 K bias with respect to the model first guess, and NOAA-16 measurements a -0.6 K bias. SEVIRI CSRs in the 6.2μm channel have a -1.7 K bias using flat RTTOV coefficients and -1.6 K using Planck weighted coefficients. This consistency gives us more confidence in the radiative transfer calculation. The difference between SEVIRI and HIRS is still significant when compared to the difference between different HIRS instruments, but is not overwhelming. The source of this bias is unclear.

First guess departure standard deviation lies at around 1.5 K for SEVIRI and NOAA-17 HIRS. For NOAA-16 HIRS this appears to be a little higher at 1.7 K.

Figure 9 shows model first guess departures for the 7.3μm channel and HIRS channel 11. The HIRS measurements both have a 0.4 K bias with respect to the model first guess. SEVIRI CSRs in the 7.3μm channel have a 0.8 K bias using flat RTTOV coefficients, and 0.5 K using Planck weighted coefficients. The biases of the two instrument types are therefore in relatively close agreement. The SEVIRI data have an unexplained diurnal variation with peak-to-peak amplitude 0.4 K. A similar variation is not seen in the HIRS first guess departure.

All three instruments show a first guess departure standard deviation of about 1.2 K.

3.4 8.7 μm channel

As mentioned above, the SEVIRI 8.7 μm channel has no analogue on the HIRS instrument, so a cross calibration is not possible. However, a comparison of the simulation of this channel using the two RTTOV coefficient files is still possible. Figure 10 shows this comparison. The two methods of simulation appear to agree very closely.

3.5 Ozone channels

HIRS and SEVIRI both carry a channel sensitive to ozone at around 9.7μm. Figure 11 shows the spectral response functions of these channels. The HIRS channel is sensitive to slightly longer wavelengths and the

SEVIRI channel to slightly shorter wavelengths, with the SEVIRI channel slightly wider than the HIRS channel. One would expect a similar response from both channels.

Figure 12 shows the mean (OBS-FG) for the ozone channels. The NOAA-16 HIRS channel shows a varying bias of between -0.5 K and -1.0 K for the period shown, while the NOAA-17 bias is more constant at around -1.0 K. The SEVIRI channel shows a mean bias of about -1.0 K for both simulation methods. The SEVIRI channel is therefore in close agreement with the HIRS channel. Standard deviations of (OBS-FG) also agree closely.

3.6 Window channels

The HIRS window channels are considerably narrower than the SEVIRI window channels – see figure 13. However, the lack of significant features in this region of the spectrum suggests that these channels should behave in a similar manner.

Figure 14 shows the biases for SEVIRI's 10.8 μm channel and HIRS channel 8 with respect to the ECMWF IFS. The HIRS channels on both NOAA-16 and -17 shows a bias of about -1.2 K. SEVIRI shows a bias of about -0.3 K regardless of simulation method used. In the absence of atmospheric interaction the difference between the instruments must either lie in the cloud clearing method used or in the satellite calibration method. As window channels are very sensitive to cloud at all levels the former is likely. Indeed, if SEVIRI data are not restricted to 100% clear the 10.8 μm channel departure is around 0.9 K (not shown); this shows that some cloud is not being detected in the creation of the CSR product. It is possible the same is true for the HIRS cloud clearing, especially as this is tuned towards the assimilation of channels insensitive to low level cloud.

Standard deviation of (OBS-FG) is low for both HIRS and SEVIRI; around 0.9 K for HIRS and 0.6 K for SEVIRI. The lower value for SEVIRI may be indicative of better cloud clearing.

Figure 15 shows the mean (OBS-FG) series for SEVIRI's 12.0μm channel and HIRS channel 10. The NOAA-16 HIRS channel shows a bias of -1.2 K, while the NOAA-17 HIRS channel shows a bias of -1.4 K. The SEVIRI channel has a bias of about -0.2 K with respect to the ECMWF IFS. This could once more be indicative of poor low level cloud clearing for HIRS. Once again the standard deviation for HIRS is marginally higher than for SEVIRI (0.9 K for HIRS, 0.7 K for SEVIRI).

3.7 13.4 μm channel

Figure 16 shows the spectral response functions for SEVIRI's 13.4 μm channel and HIRS channel 18. Again the HIRS channel is considerably narrower, suggesting a tighter weighting function.

Figure 17 shows the mean (OBS-FG) for these channels. The HIRS channels on both NOAA-16 and -17 are on average 0.5 K colder than the model. The MSG is unbiased with respect to the model using flat RTTOV coefficients. It has a bias of 0.5 K using Planck weighted coefficients. The bias is also sensitive to the clear percentage of the CSR, with a bias of -0.5 K if all data are used with flat RTTOV coefficients. All this suggests that the difference between these instruments may be adequately explained by errors in modelling or differences in cloud clearing. Standard deviations are around 0.8 K for HIRS and 0.6 K for SEVIRI, again suggesting more cloud contamination for HIRS.

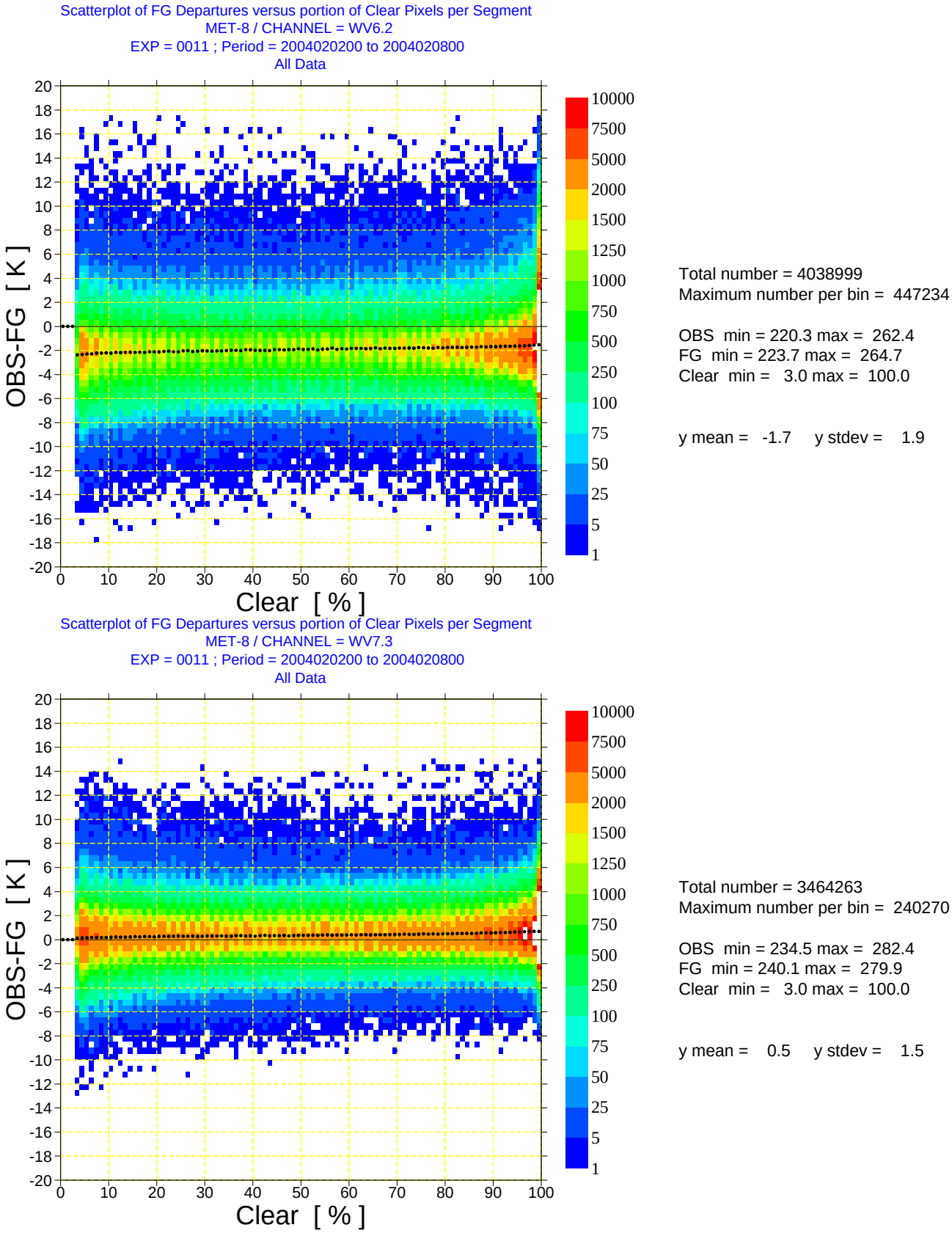

Figure 3: Scatterplot of observation minus first guess for Meteosat-8 6.2 μm channel (top) and 7.3 μm channel (bottom) against percentage of clear pixels per segment.

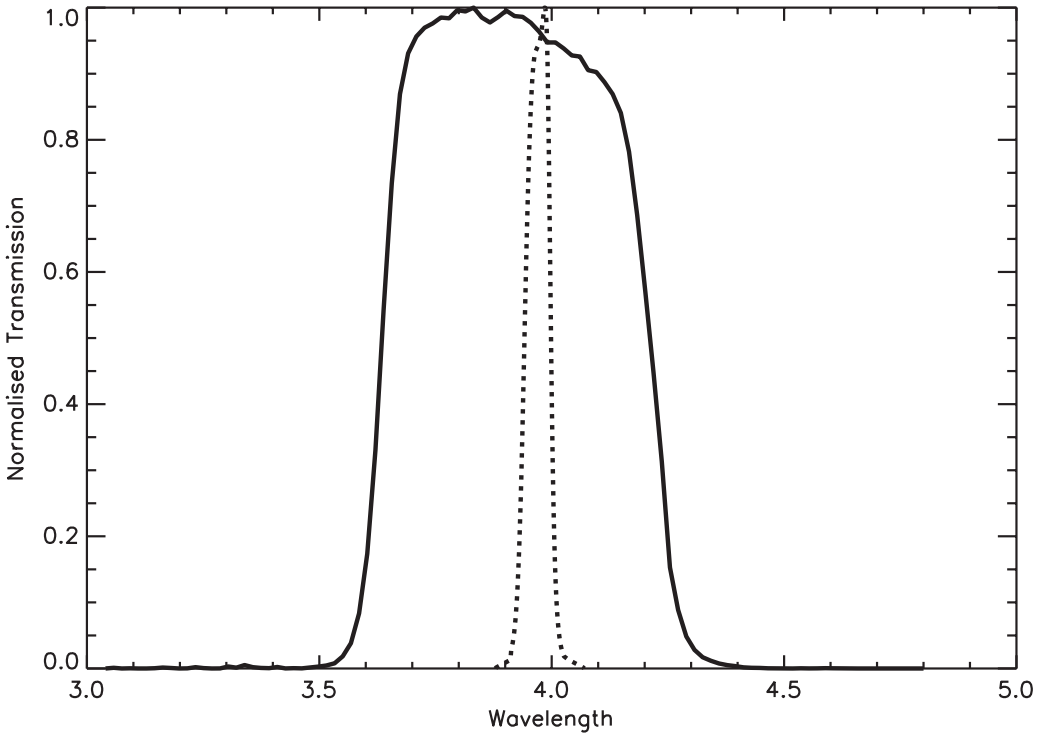

Figure 4: Meteosat-8 SEVIRI 3.9 μm channel (solid) and NOAA-17 HIRS channel 18 (dotted) spectral response functions.

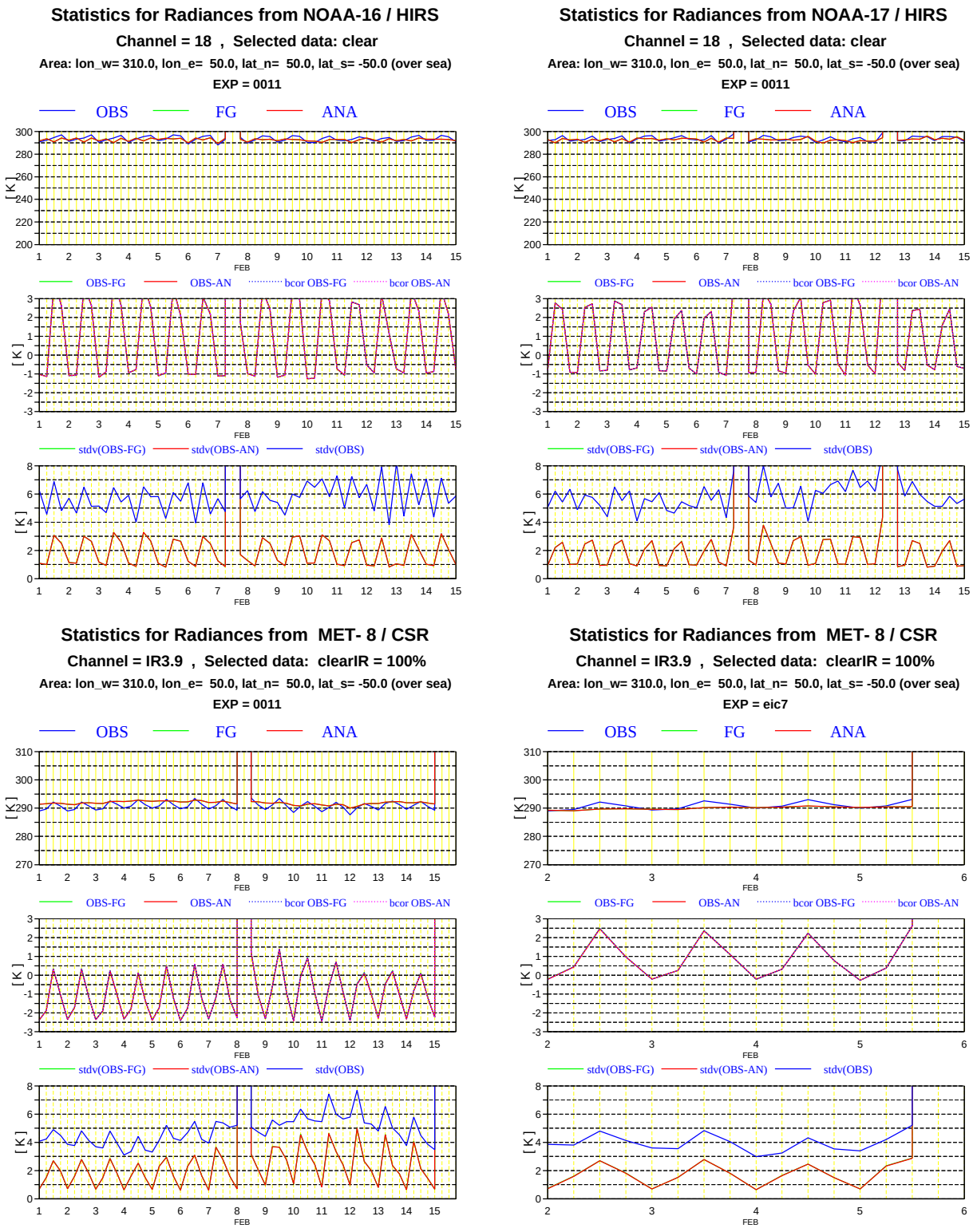

Figure 5: First guess departure of NOAA-16 and -17 HIRS channel 18 (top left and right panels respectively) and Meteosat-8 3.9μm channel using flat and Planck weighted RTTOV coefficients (bottom left and right panels respectively). All data are over sea. Cloud free data are selected for HIRS and 100% clear data for SEVIRI.

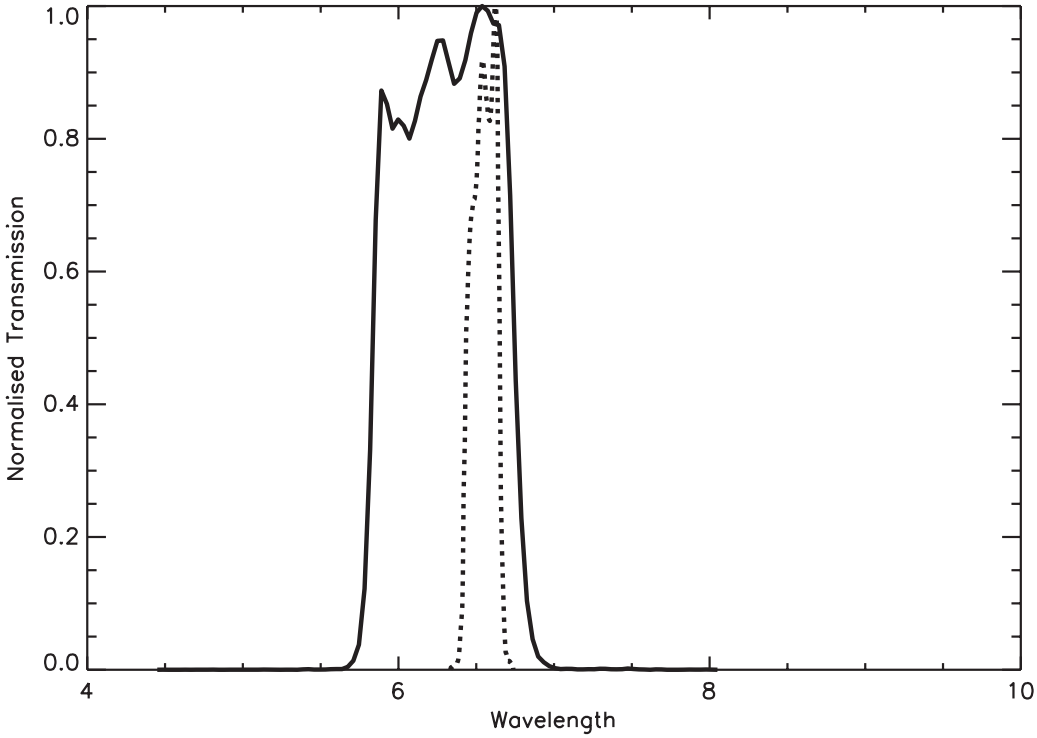

Figure 6: Meteosat-8 SEVIRI 6.2 μm channel (solid) and NOAA-17 HIRS channel 12 (dotted) spectral response functions.

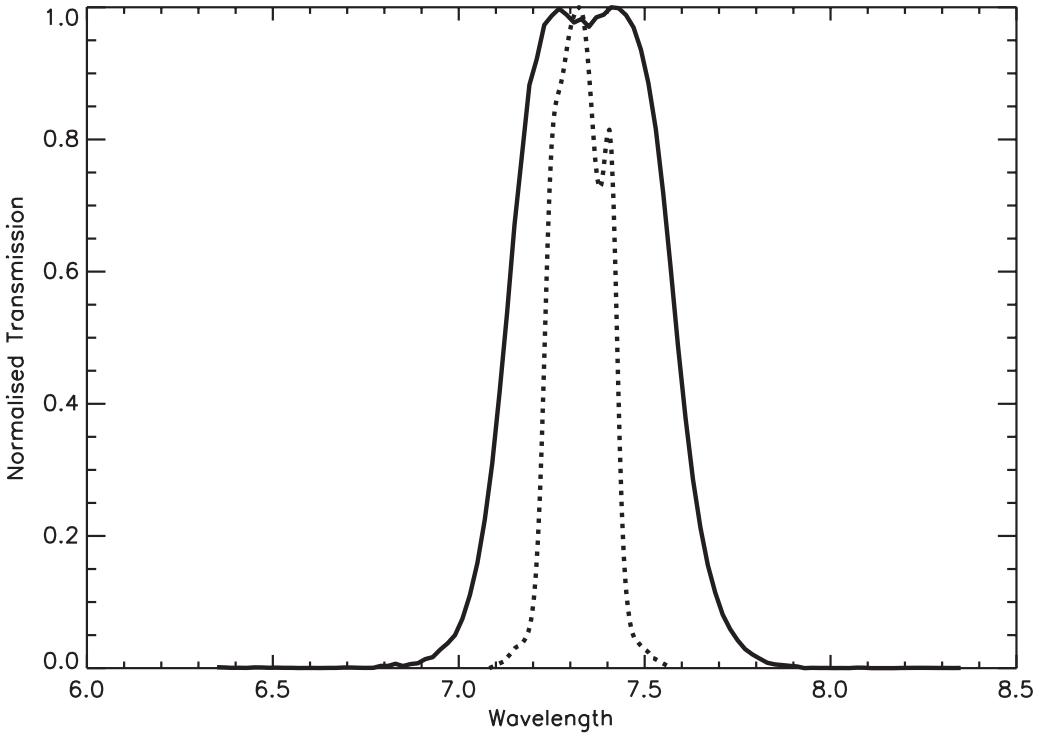

Figure 7: Meteosat-8 SEVIRI 7.3 μm channel (solid) and NOAA-17 HIRS channel 11 (dotted) spectral response functions.

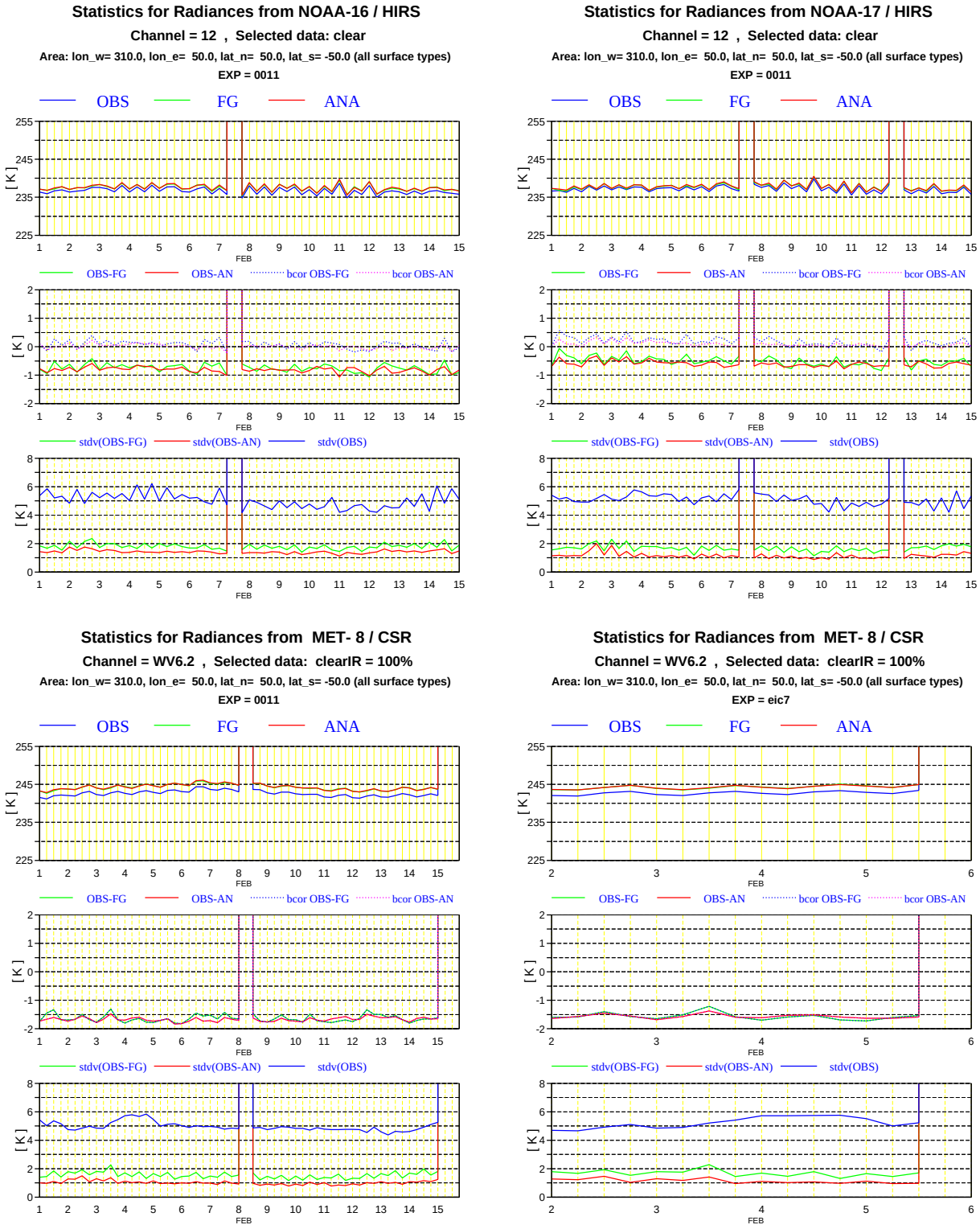

Figure 8: First guess departure of NOAA-16 and -17 HIRS channel 12 (top left and right panels respectively) and Meteosat-8 6.2 μm channel with flat and Planck weighted RTTOV coefficients (bottom left and right panel respectively). Cloud free data are selected for HIRS and 100% clear data for SEVIRI.

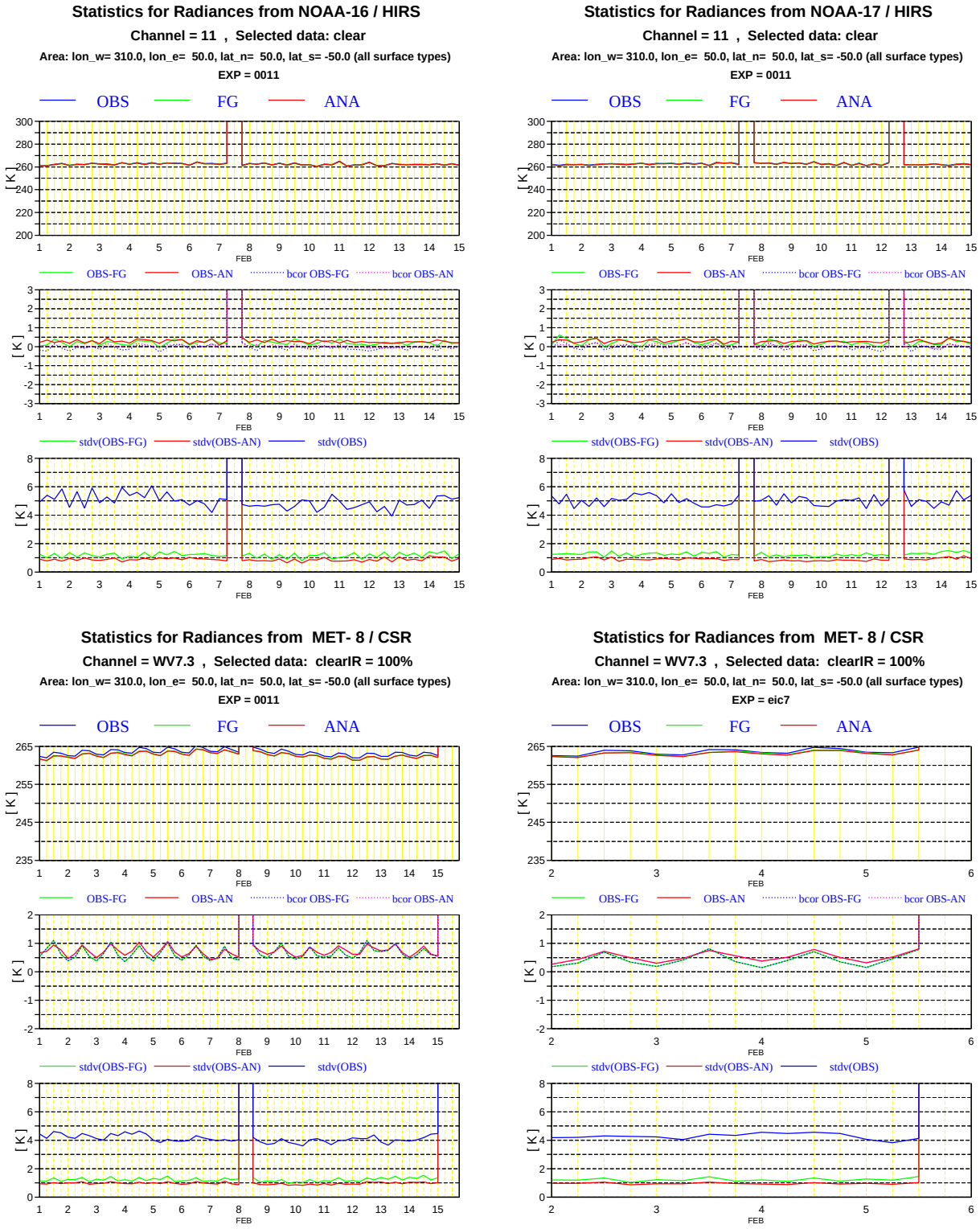

Figure 9: First guess departure of NOAA-16 and -17 HIRS channel 11 (top left and right panels respectively) and Meteosat-8 7.3 μm channel with flat and Planck weighted RTTOV coefficients (bottom left and right panel respectively). Cloud free data are selected for HIRS and 100% clear data for SEVIRI.

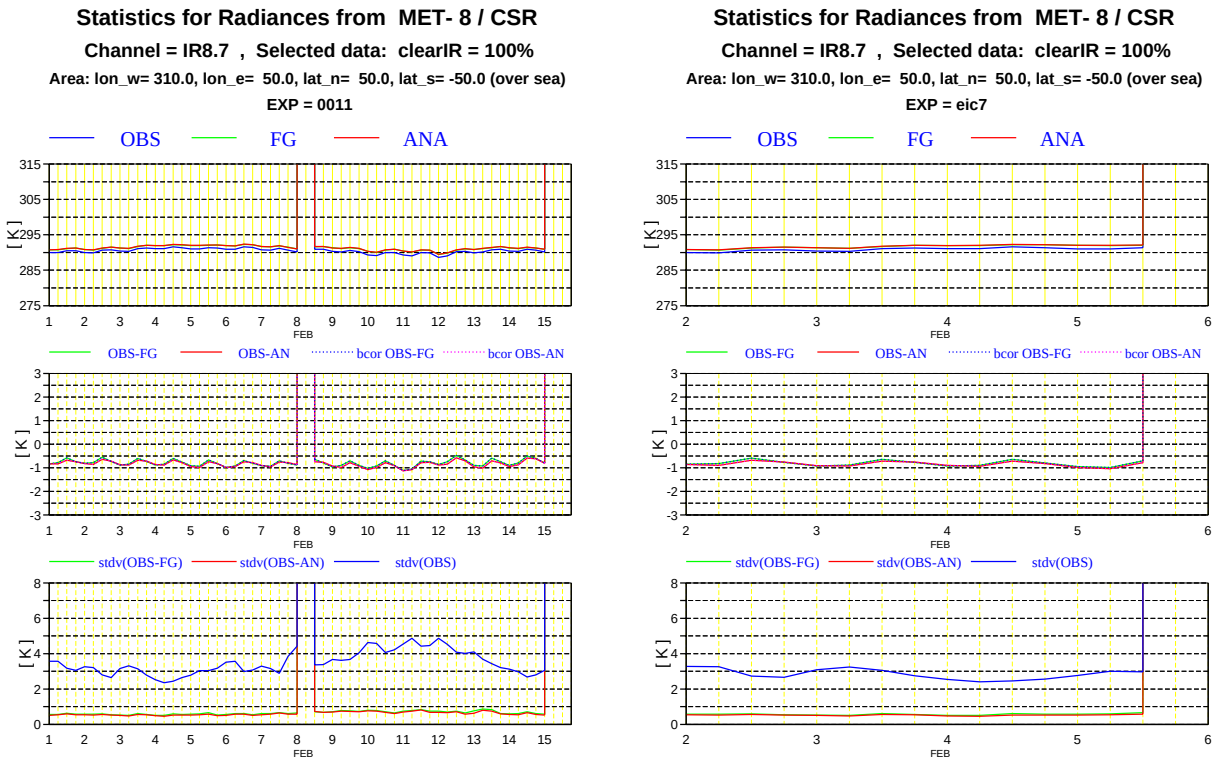

Figure 10: First guess departure of Meteosat-8 8.7 μm channel using flat and Planck weighted RTTOV coefficients. All data are over sea and 100% clear.

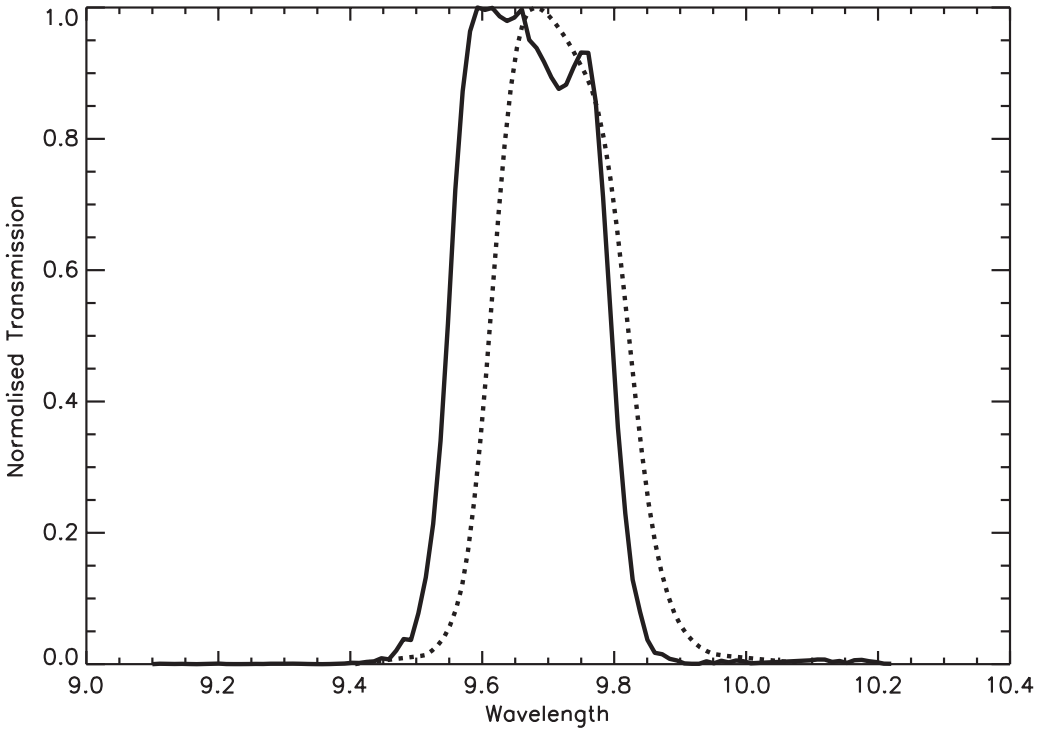

Figure 11: Meteosat-8 SEVIRI 9.7 μm channel (solid) and NOAA-17 HIRS channel 9 (dotted) spectral response functions.

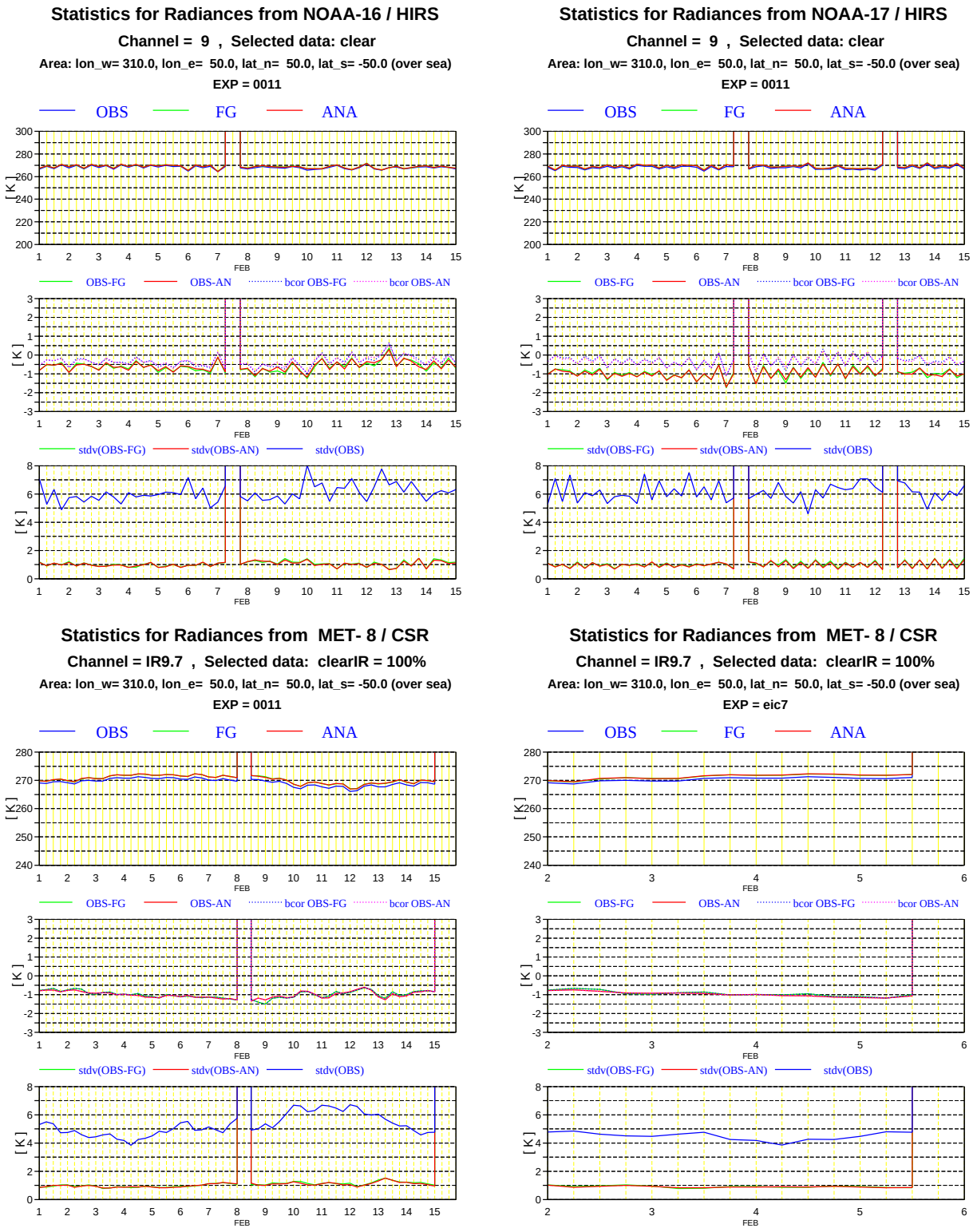

Figure 12: First guess departure of NOAA-16 and -17 HIRS channel 9 (top left and right panels respectively) and Meteosat-8 9.7 μm channel using flat and Planck weighted RTTOV coefficients (bottom left and right panels respectively). All data are over sea. Cloud free data are selected for HIRS and 100% clear data for SEVIRI.

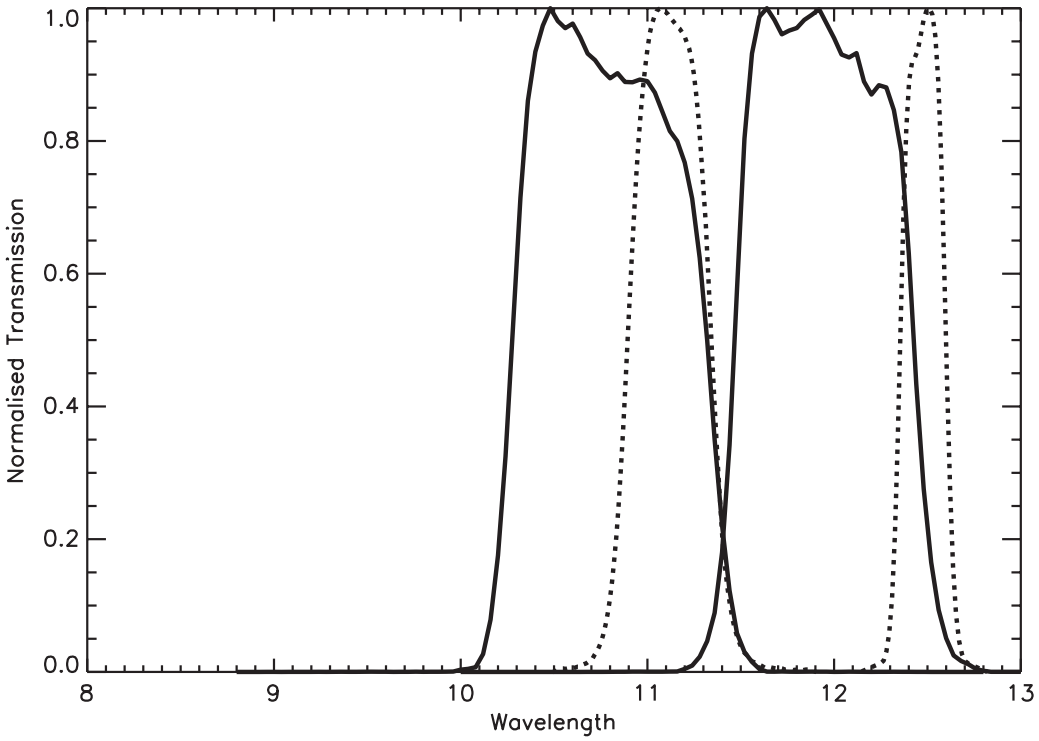

Figure 13: Meteosat-8 SEVIRI window channel (solid) and NOAA-17 HIRS channel 8 and 10 (dotted) spectral response functions.

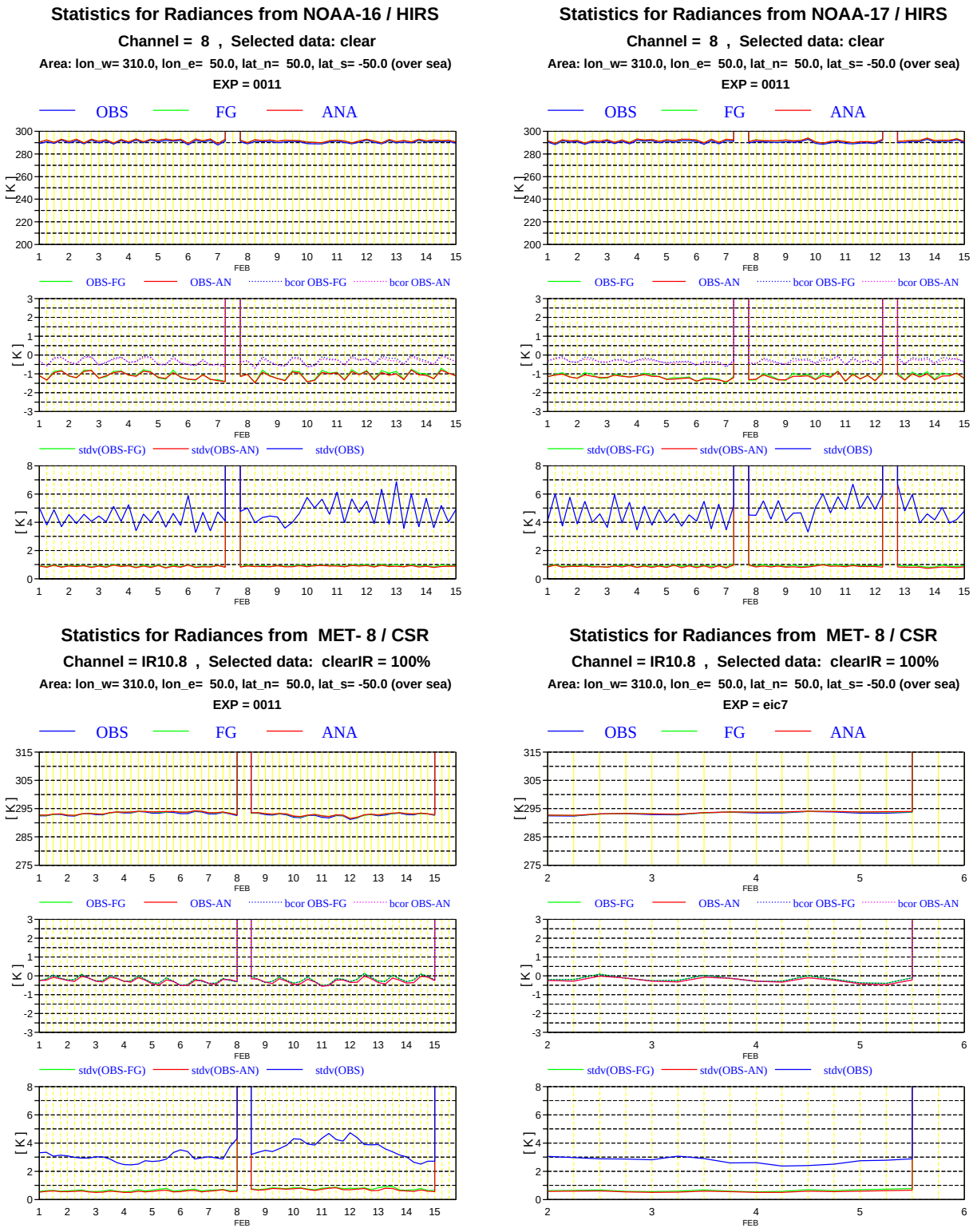

Figure 14: First guess departure of NOAA-16 and -17 HIRS channel 8 (top left and right panels respectively) and Meteosat-8 10.8 μm channel using flat and Planck weighted RTTOV coefficients (bottom left and right panels respectively). All data are over sea. Cloud free data are selected for HIRS and 100% clear data for SEVIRI.

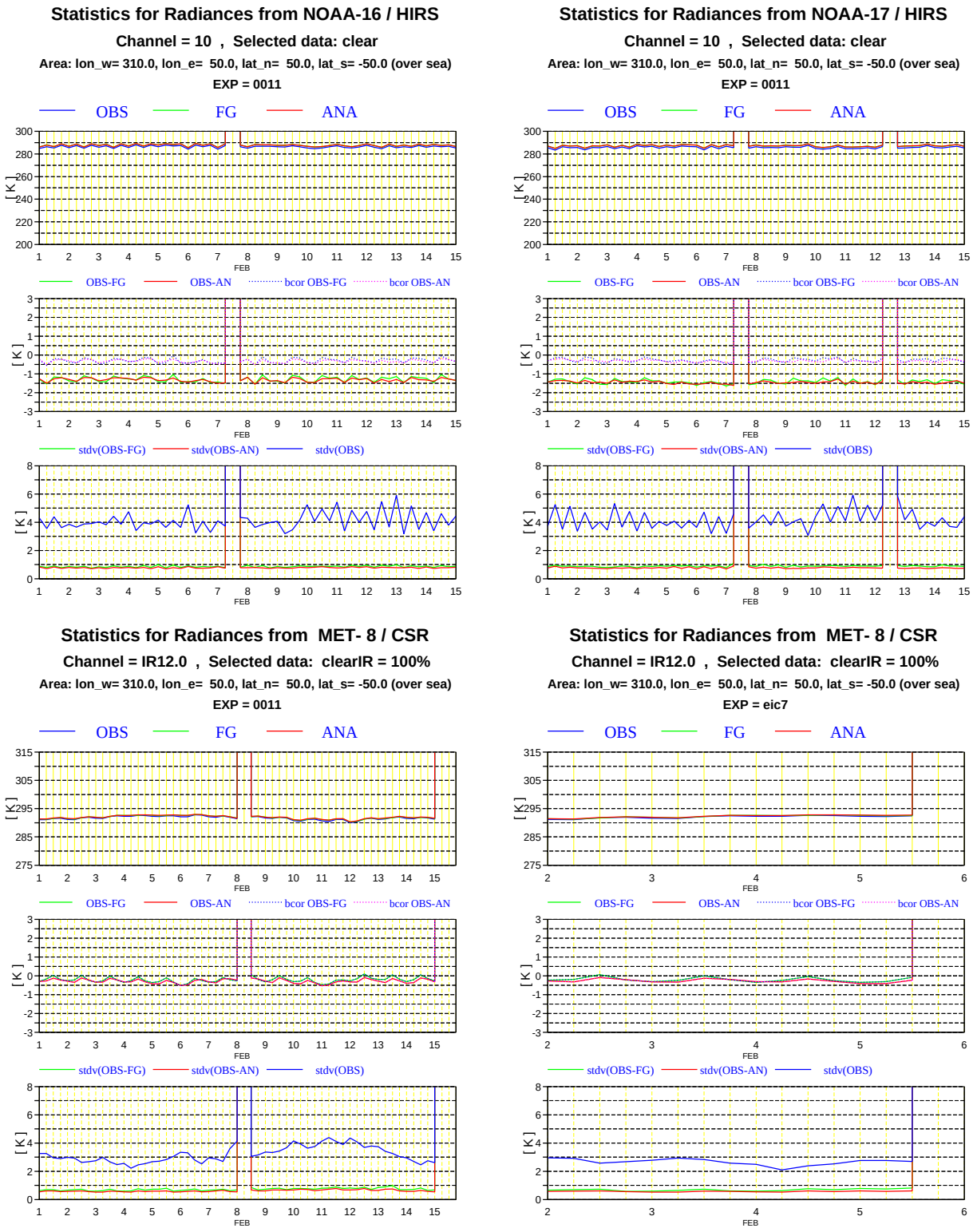

Figure 15: First guess departure of NOAA-16 and -17 HIRS channel 10 (top left and right panels respectively) and Meteosat-8 12.0 μm channel using flat and Planck weighted RTTOV coefficients (bottom left and right panels respectively). All data are over sea. Cloud free data are selected for HIRS and 100% clear data for SEVIRI.

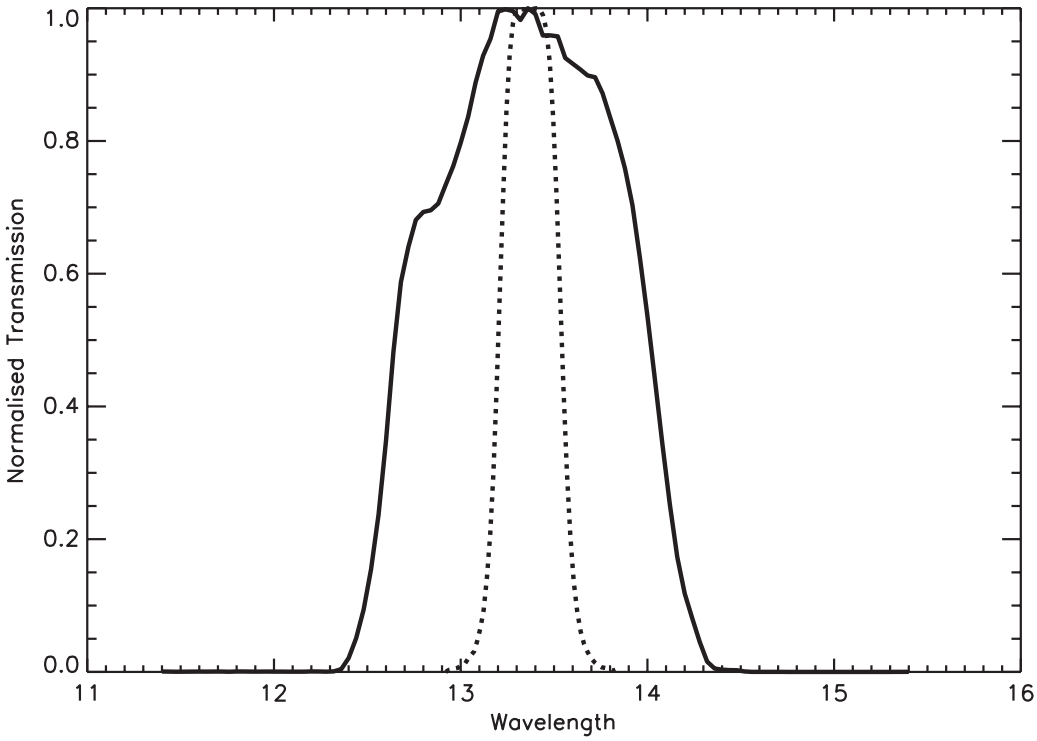

Figure 16: Meteosat-8 SEVIRI 13.4 μm channel (solid) and NOAA-17 HIRS channel 7 (dotted) spectral response functions.

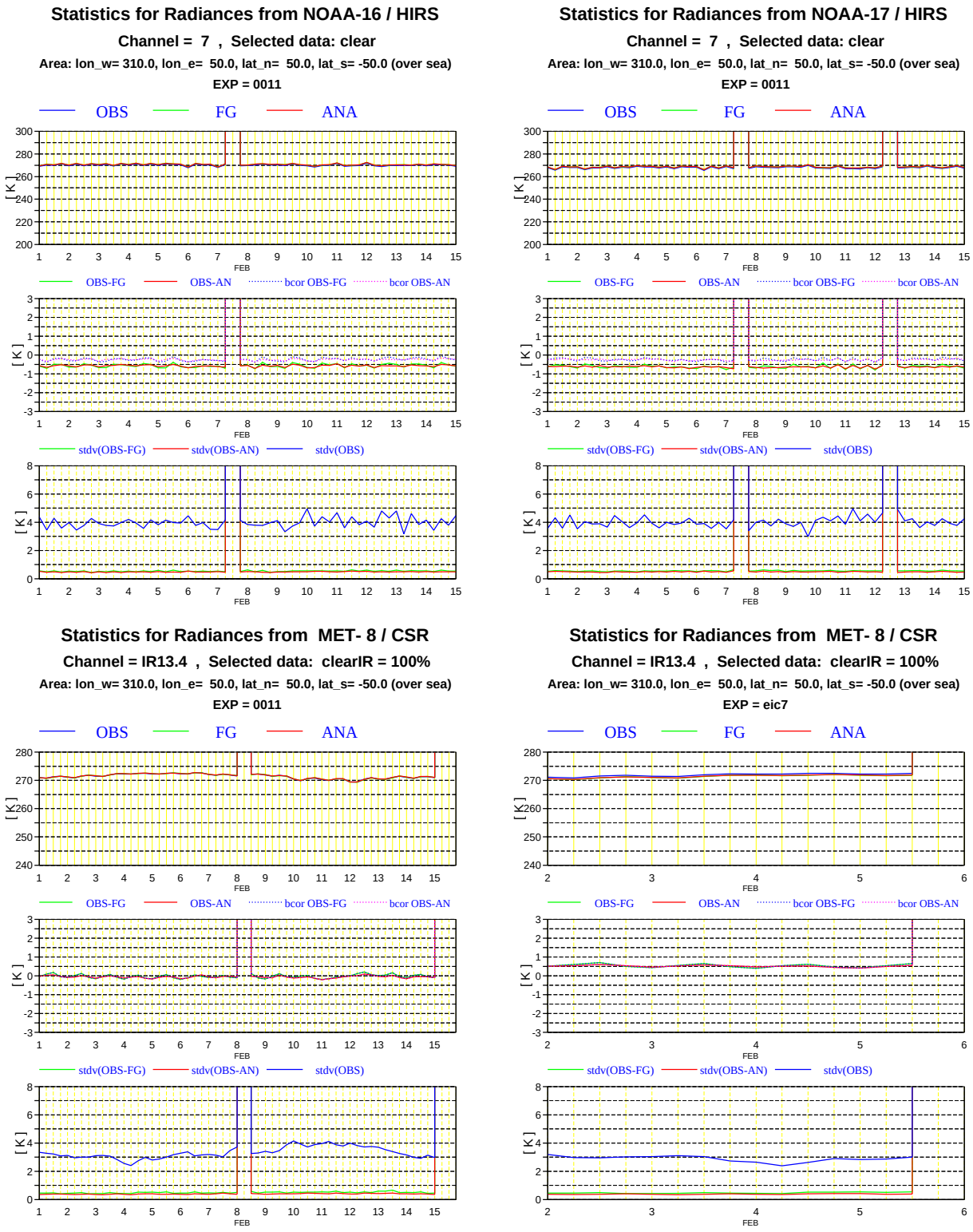

Figure 17: First guess departure of NOAA-16 and -17 HIRS channel 7 (top left and right panels respectively) and Meteosat-8 13.4 μm channel using flat and Planck weighted RTTOV coefficients (bottom left and right panels respectively). All data are over sea. Cloud free data are selected for HIRS and 100% clear data for SEVIRI.

4 Assimilation Strategy

Two assimilation trials were carried out. In both trials Meteosat-7 data were blacklisted to avoid the use of similar data for similar locations. A control run was made with both Meteosat-7 and -8 blacklisted. Operational data including Meteosat-7 were also used for control purposes; see below. For the Meteosat-8 trial runs only the water vapour channels 6.2 μm and 7.3 μm were assimilated. In the first trial, hereafter referred to as trial SEVIRI 1, both channels were assigned an error of 2.0 K. In the second trial, referred to as trial SEVIRI 2, the 7.3 μm channel was assigned an error of 1.5 K and the 6.2 μm channel an error of 2.0 K. Unlike the MVIRI data from the Meteosat series of satellites, there is no evidence of solar stray light intrusion degrading data away from the very edge of a SEVIRI image. As a result we did not blacklist data at local midnight. We did blacklist data over ground higher than 1.5 km, data from zenith angles greater than 60° and, in light of the above comments about cloud contamination, all data with a clear percentage of less than 70%.

The SEVIRI data used were bias corrected in a similar manner to that outlined by Harris and Kelly. The differences in method are that we used only 3 predictors in our regression (1000 hPa to 300 hPa thickness, 200 hPa to 50 hPa thickness and total column water vapour) and we applied no scan correction to the observations.

These two experiments and the control were run from 2nd February 2004 until 2nd March 2004 using initial data from the ‘esuite’, the operational testbed for the new operational suite which was running in February 2004, giving a 30 case trial. This esuite was also used as an alternative control with the Meteosat-7 data assimilated. All experiments were run at full resolution (i. e. T511 forecast run and T159 assimilation) using 4D-Var based on ECMWF’s Integrated Forecast System (IFS) cycle 28 revision 1.

5 Analysis increments

An examination of the analysis increments shows that the assimilation of SEVIRI data has a significant impact on both humidity and upper tropospheric winds field analysis. Little impact is seen on lower tropospheric winds; this is at least in part due to the lower background error of lower tropospheric winds.

Figures 18, 19 and 20 show cross-sections of the difference in increment in relative humidity due to the assimilation of Meteosat-7 and Meteosat-8 water vapour radiances. The cross-sections run through the 0° meridian, are for one cycle only and use the same initial condition. These figures show us that the use of SEVIRI data gives us larger increments and increments with more vertical structure. The increase in increment strength is likely to be due to the fact that twice as many observations are being used; we use two SEVIRI channels and only one MVIRI channel. If both channels make similar observations then there will be a stronger increment, as the two SEVIRI channels have weighting functions which, whilst peaking at different heights, are both broad. Only small differences may be observed between the increments shown in figures19 and 20.

Figures 21, 22 and 23 show the vector wind increments at 300 hPa due to the assimilation of MVIRI and SEVIRI water vapour radiance data. The main difference between these figures is the extent of the area over which the winds are modified; SEVIRI data lead to a wider area of modification than MVIRI data. Again, SEVIRI assimilation method does not change the broad nature of the increments although it does subtly alter the increment.

6 Forecast skill

The assimilation of SEVIRI water vapour radiances improves the fit of radiosonde humidity data; figure24 shows that the biases of sonde humidity data against both the background and analysis are reduced.

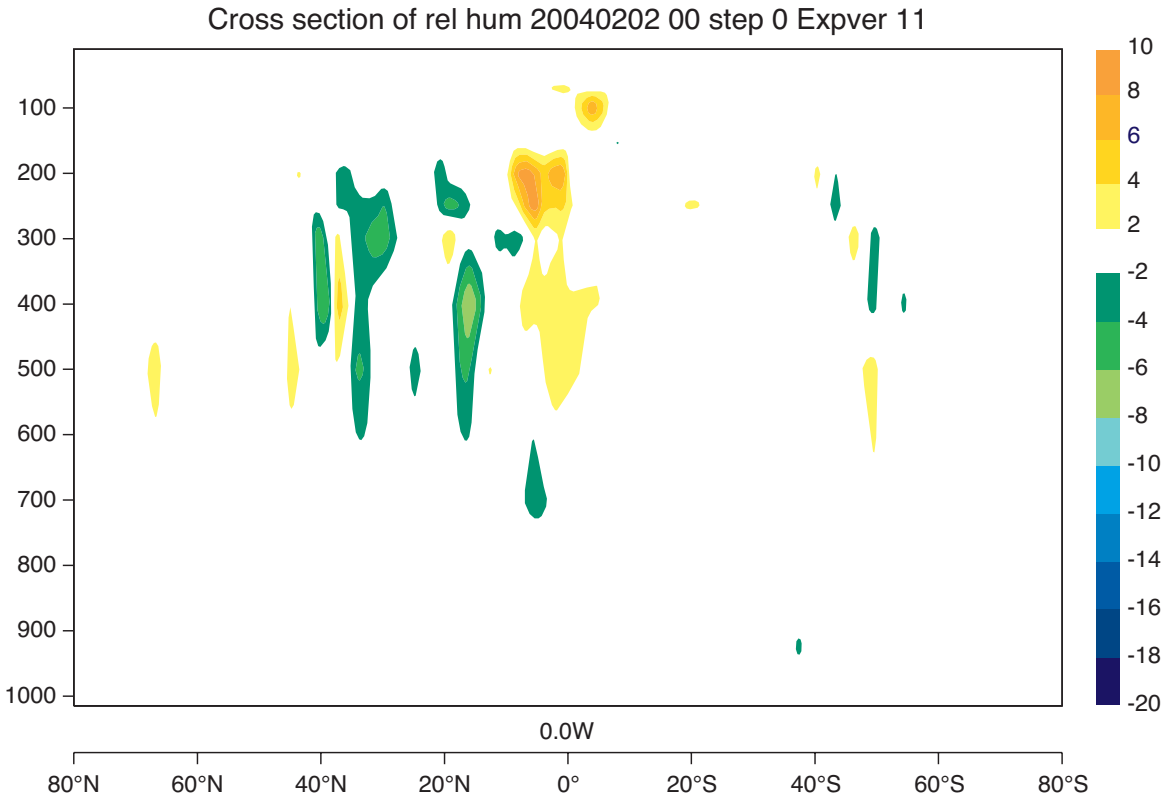

Figure 18: Cross-section of difference in relative humidity increment for first analysis due to Meteosat-7 CSR assimilation at 0^{o}W.

The fit of AMSU-B data from NOAA-16 are also improved by the assimilation of SEVIRI water vapour data. Figure 25 shows the difference between standard deviation of first guess departure of AMSU-B channel 3 on NOAA-16 for trial SEVIRI 1 and for control. The area observed by Meteosat-8 is clearly discernable, showing that the assimilation of SEVIRI data reduces the standard deviation of first guess departure in this upper tropospheric humidity channel. The equivalent figure for another upper tropospheric humidity channel, HIRS channel 12, shows a similar result – see figure 26.

The impact of MSG observations is most readily seen on lower tropospheric tropical wind forecast skill. Figure 27 shows RMSE in vector wind for all experiments; it is not clear which experiment is best without further statistical analysis, but the Meteosat-8 experiment with equal variance for both assimilated channels (trial SEVIRI 1) looks most promising in the 5 to 8 day forecast range.

Statistical analysis of the vector wind scores bears out the initial impressions taken from figure 27. Table 1 gives t-test significances for the impact of Meteosat-8 SEVIRI assimilation with $\mathbf{R} = diag(4.0, 4.0)$ K^2 on vector wind RMSE when compared to the control run, and shows evidence of improved skill for both low level vector winds and 300 hPa vector winds.

Anomaly correlation plots for height fields give little information about the skill of Meteosat-8 assimilation, although there is some indication of a slight negative impact on southern hemisphere height fields from Meteosat-7 assimilation over the period of this experiment (comparing the control and the esuite). Significance tests show a positive impact on northern hemisphere upper tropospheric height fields during this experiment – table 2 gives t-test significances for height field impact in the same experiment as table 1.

Figure 28 shows the difference in anomaly correlation for various height fields between trial SEVIRI 1 and

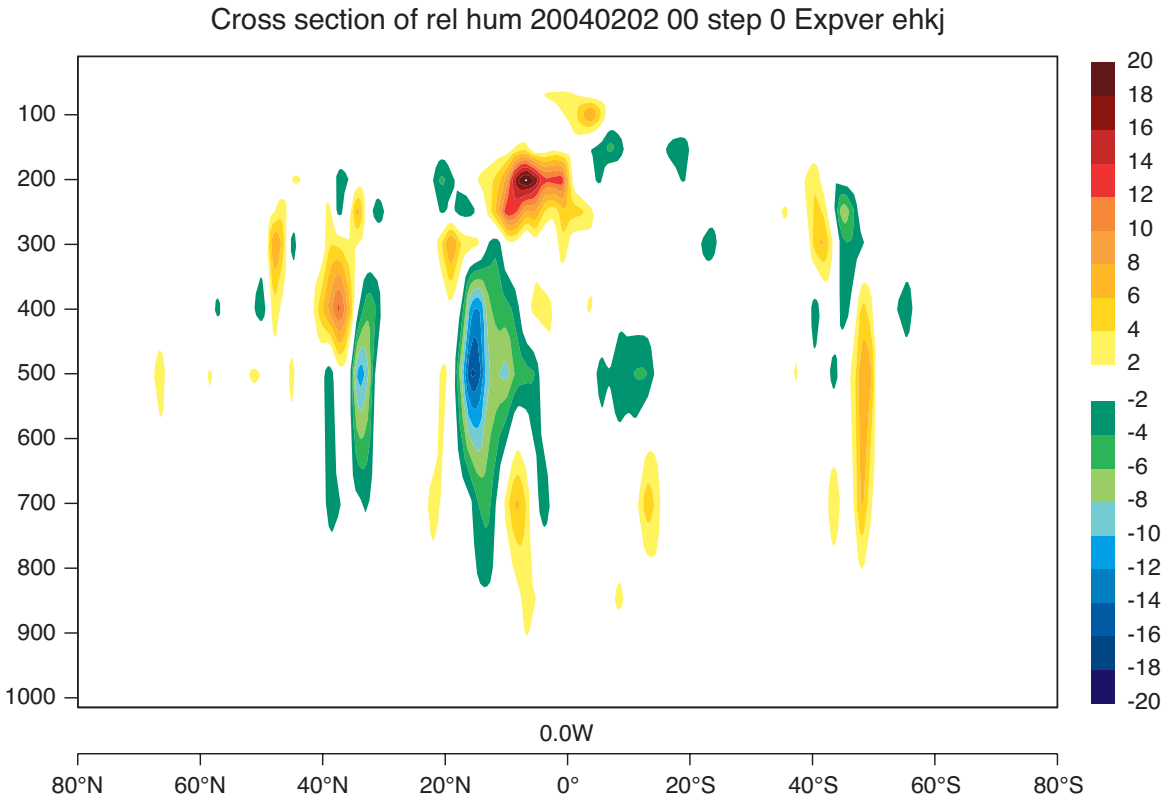

Figure 19: As figure 18 for Meteosat-8 data assimilation with error of 2 K in both water vapour channels.

Forecast Range (Days)	2	3	4	5	6	7
1000 hPa, Tropics	–	–	–	95% ?	99.5% ?	99.8% ?
850 hPa, Tropics	– ?	–	90%	95%	98% ?	99.5% ?
500 hPa, Tropics	–	–	–	–	–	99%
300 hPa, Tropics	95%	99.5%	95%	95%	95%	98%

Table 1: t-test significance of impact on RMSE in vector wind. All impacts were positive, – denotes no impact of significance 90% or greater. A question mark indicates that a significant correlation or anti-correlation between cases was detected, throwing doubt on the validity of the t-test.

the control. Positive values imply positive impact for trial SEVIRI 1. In the northern hemisphere the mean difference is always positive (i.e. Meteosat-8 assimilation gives positive impact) although this is only 95% significant for 4-6 day forecasts. In the southern hemisphere the mean is positive to day 6 forecasts and negative beyond that range, although 95% significance is not achieved until day 9, by which time both forecasts have little skill.

Figure 29 is the equivalent of figure 28 but verified against operations (i.e. control experiment + Meteosat-7 assimilation). This comparison shows us that for this period we can be 95% confident that trial SEVIRI 1 gives superior forecasts of upper tropospheric height fields for days 3 to 5. Results are neutral at other ranges and in the southern hemisphere.

Figure 30 is the equivalent of figure 28 but verified against the alternative Meteosat-8 assimilation trial, SEVIRI 2. In the northern hemisphere trial SEVIRI 1 appears to give superior forecasts at most ranges, although not sufficiently superior to give 95% certainty except for the 24 hour forecast where trial SEVIRI 2 appears to be

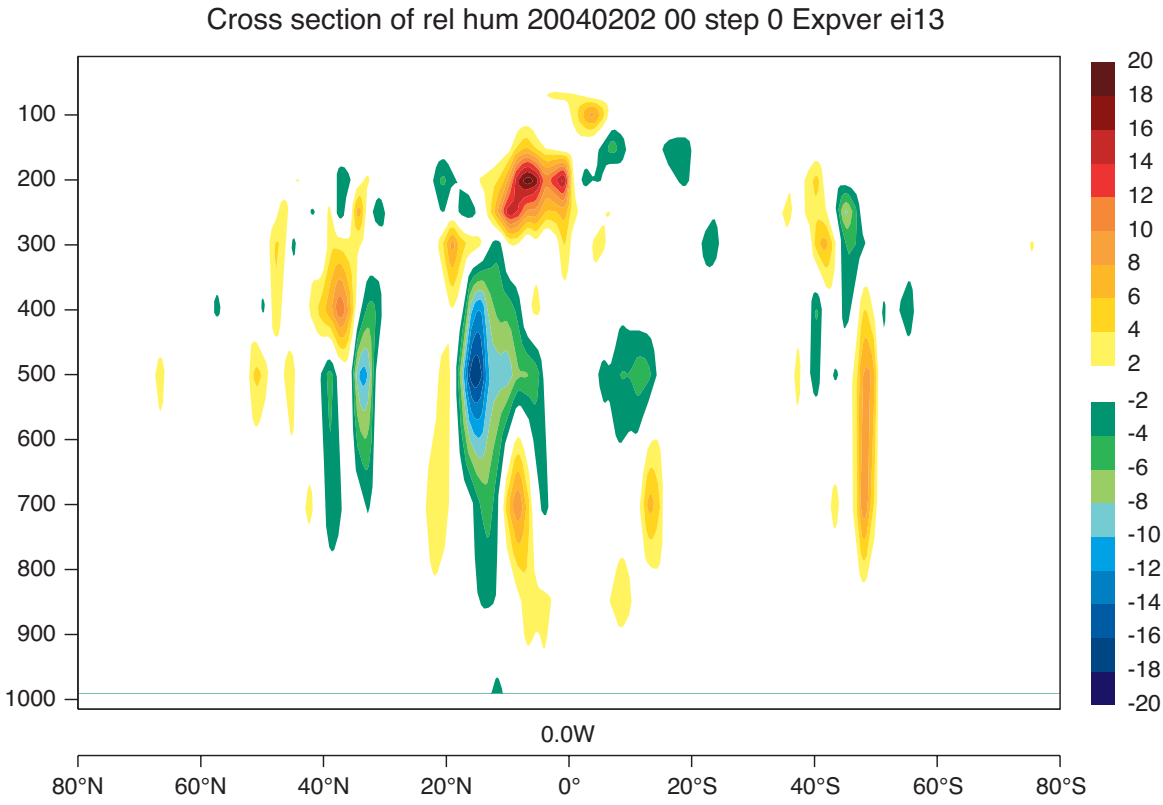

Figure 20: As figure 18 for Meteosat-8 data assimilation with error of 2 K in 6.2 μm channel and 1.5 K in 7.3 μm channel.

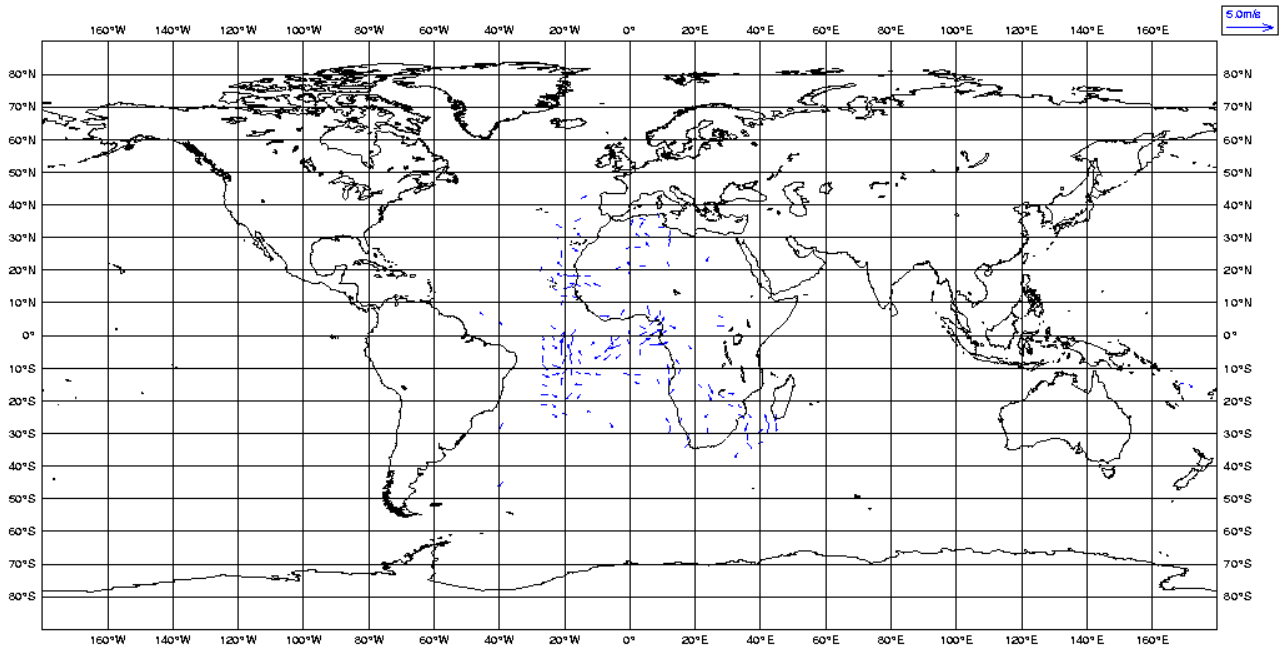

Figure 21: Difference in 300 hPa vector wind increment for first analysis due to Meteosat-7 CSR assimilation.

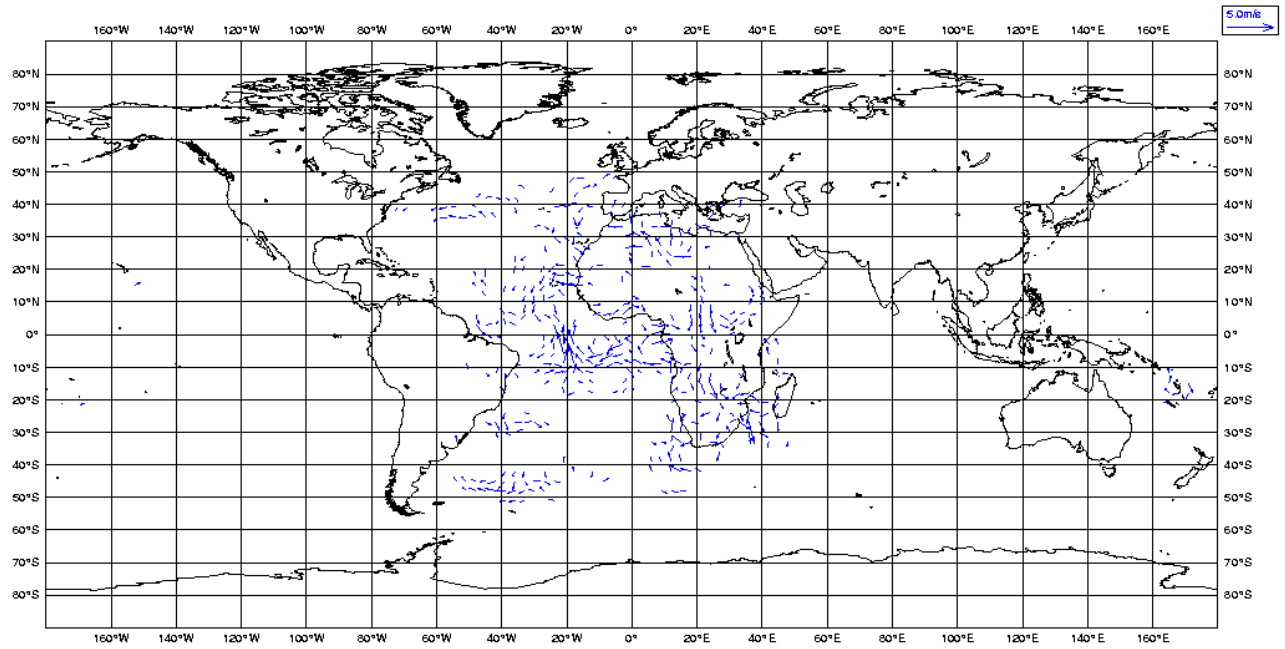

Figure 22: As figure 21 for Meteosat-8 data assimilation with error of 2 K in both channels.

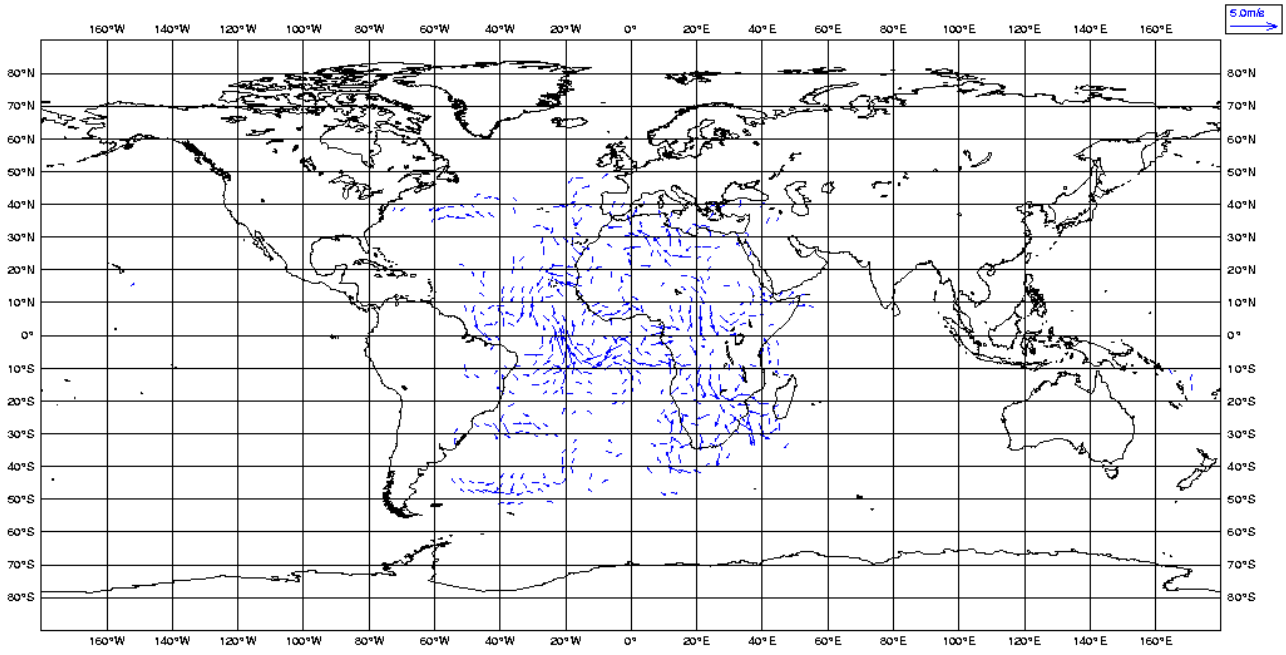

Figure 23: As figure 21 for Meteosat-8 data assimilation with error of 2 K in 6.2 μm channel and 1.5 K in 7.3 μm channel.

superior with 95% certainty. In the southern hemisphere the two strategies appear to have similar skill until day 8 when trial SEVIRI 2 is better with 95% certainty, although forecasts at this range are poor for both experiments. Trial SEVIRI 2 is slightly better at range 4-5 days, but not significantly so.

Figure 31 shows the difference in RMS error for tropical vector wind field at various heights between trial SEVIRI 1 and the control. Note that negative values imply positive impact for trial SEVIRI 1. These graphs

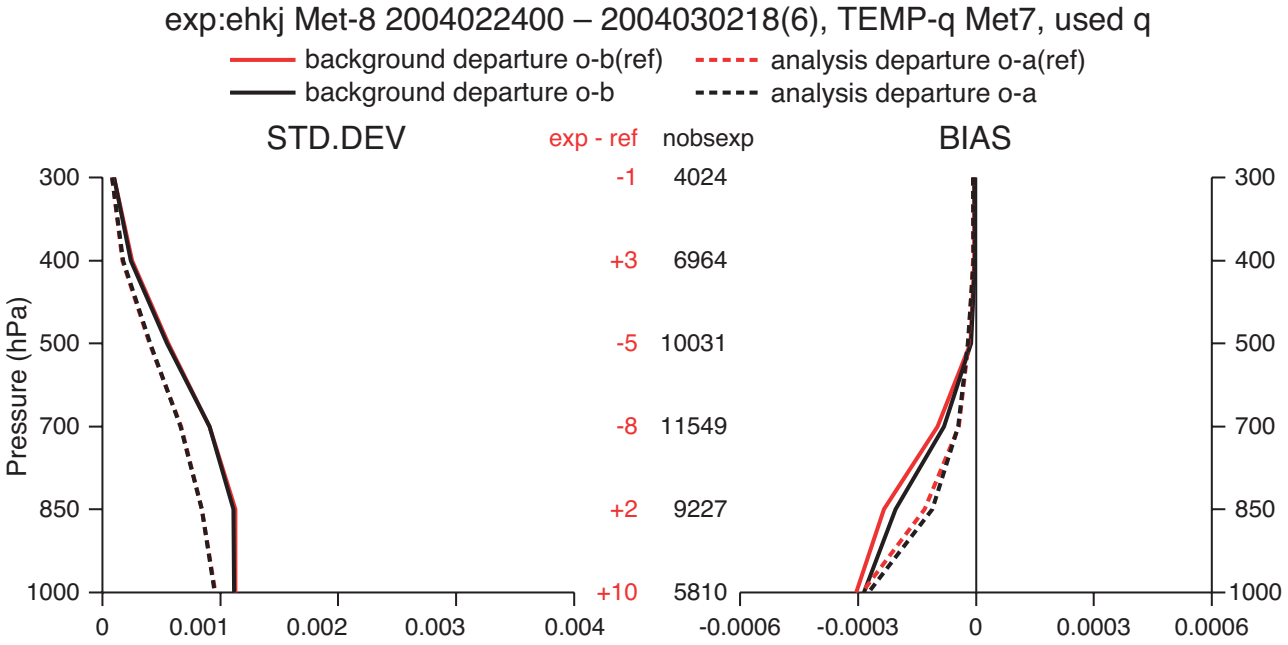

Figure 24: Standard deviation and bias in first guess and analysis departures of radiosonde humidity data (solid and dotted lines respectively) in the final week of trial SEVIRI 1 (black line) and the control experiment (red line).

Forecast Range (Days)	2	3	4	5	6	7
500 hPa, Northern Hemisphere	–	90%	98%	98%	95%	–
500 hPa, Southern Hemisphere	–	–	–	– ?	–	– ?
300 hPa, Northern Hemisphere	–	90%	99%	99.5%	95%	–
300 hPa, Southern Hemisphere	–	–	–	–	–	–

Table 2: t-test significance of impact on height field anomaly correlation. All impacts were positive, – denotes no impact of significance 90% or greater. A question mark indicates that a significant correlation or anti-correlation between cases was detected, throwing doubt on the validity of the t-test.

show a mean positive impact for trial SEVIRI 1 at most ranges and heights, although some negative impact is implied at shorter ranges for near-surface winds. At 300 hPa the positive impact is consistently 95% significant for forecast ranges between 2 and 7 days.

7 Summary

The experiments described in this report show that Meteosat-8 data assimilation would have had a positive impact on wind and height field forecasts in February 2004. The improvement in wind field impact is probably attributable to a better assignment of moisture in the vertical, as implied by the greater vertical structure in the humidity increments and as a consequence of the extra water vapour channel on SEVIRI. This improvement in humidity distribution, coupled with ECMWF's 4D-Var assimilation system, will lead to a better assignment of wind increments in the vertical.

The diurnal cycle noted in the SEVIRI water vapour first guess departures is in need of further investigation;

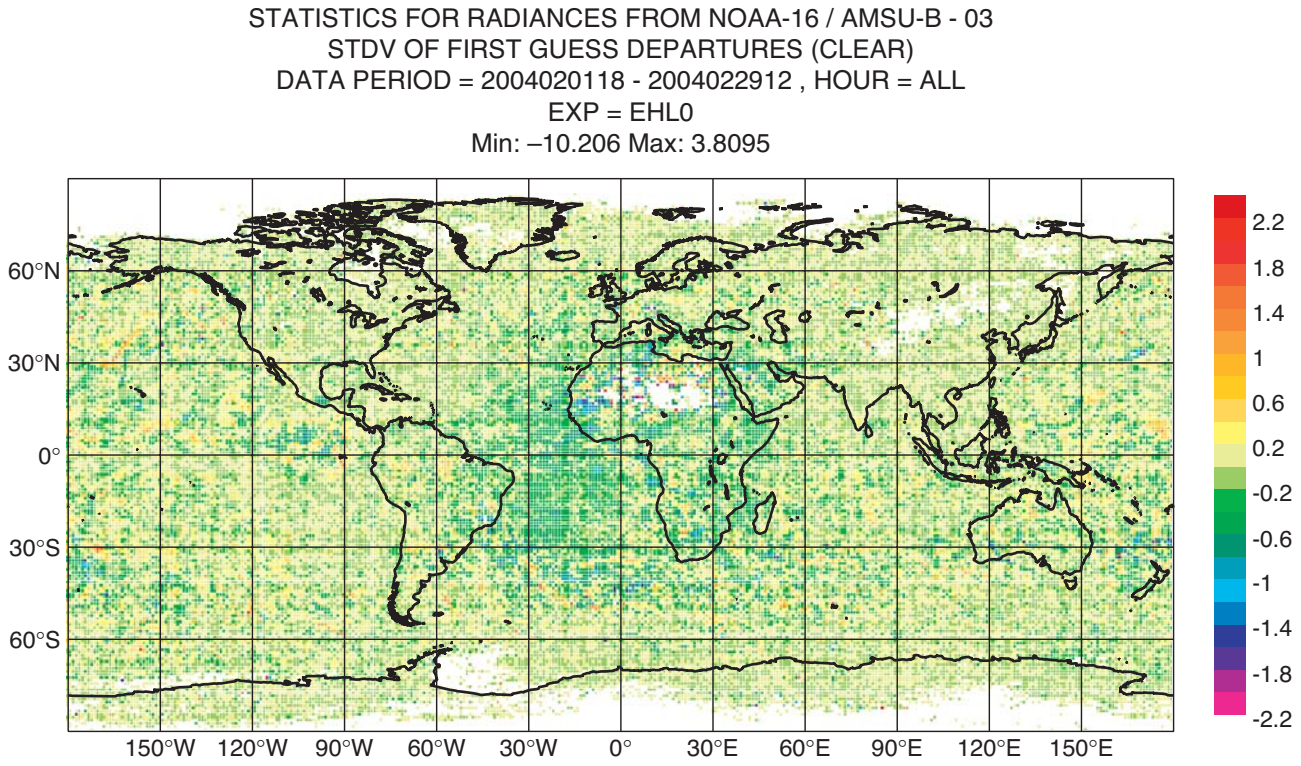

Figure 25: Difference between standard deviation of AMSU-B channel 3 first guess departure on NOAA-16 with and without SEVIRI water vapour assimilation. Greens and blues imply a better fit, yellows and reds a worse fit.

while it is possibly attributable to the diurnal nature of cloud clearing methods (i.e. use of visible channels in the daytime) and the diurnal variation of cloud, this should be confirmed. No equivalent diurnal cycle is observed in Meteosat-5 or -7 CSR product first guess departures despite a similar cloud clearing method being employed.

At present Meteosat-8 data are subject to recalibration at eclipse time and occasional alterations of cloud scheme; these changes have not impacted the quality of water vapour channel CSR data since the satellite became operational in January 2004. The data are delivered in a reliable and stable manner. The assimilation of the data from the 6.2 μm and 7.3 μm channels should improve the skill of the IFS. The preferred assimilation method is that tested in SEVIRI 1 (equal variance) as there appears to be little to choose between the two strategies tested in terms of trial forecast skill and SEVIRI 1 is the more conservative approach.

Operational assimilation of Meteosat-8 water vapour radiance data began at ECMWF on 28th September 2004.

Acknowledgements

This work was financed in the framework of the EUMETSAT/ECMWF fellowship programme. The authors would like to thank Christina Köpken for her work on clear sky radiance assimilation between 2000 and 2003; her work was the foundation upon which this work was built. At ECMWF, Milan Dragosavac and John Hodkinson have helped with data processing. At EUMETSAT, Simon Elliot, Thomas Heinemann, Kenneth Holmund and Stephen Tjemkes have all helped in the understanding and processing of this data.

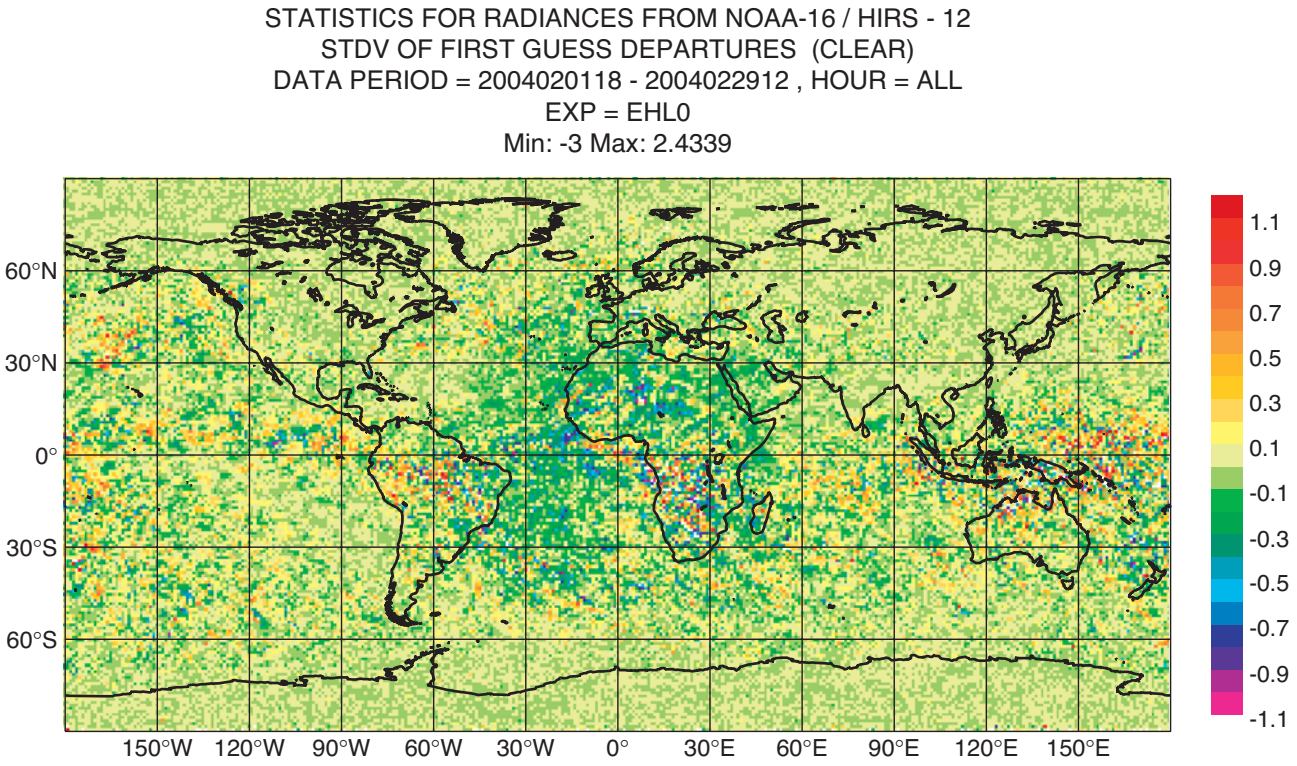

Figure 26: Difference between standard deviation of HIRS channel 12 first guess departure on NOAA-16 with and without SEVIRI water vapour assimilation. Greens and blues imply a better fit, yellows and reds a worse fit.

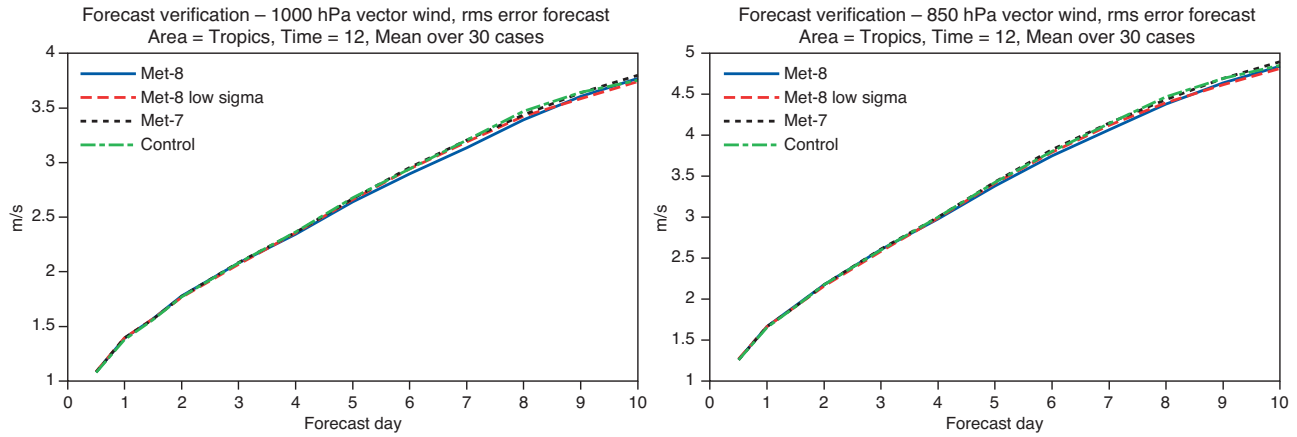

Figure 27: RMS error in vector wind at 1000 hPa (left) and 850 hPa (right) for Meteosat-8 assimilation with $\mathbf{R} = diag(4.0, 4.0)$ K^2 and $\mathbf{R} = diag(4.0, 2.25)$ K^2 strategies (labelled 'Met-8' and 'Met-8 low sigma' respectively), Meteosat-7 assimilation and the control run. 30 cases are considered.

References

Brunel, P and Saunders, R. W. *pers com*

Harris, B.A. and Kelly, G., 2001: A satellite radiance-bias correction scheme for data assimilation. *Q. J. R.*

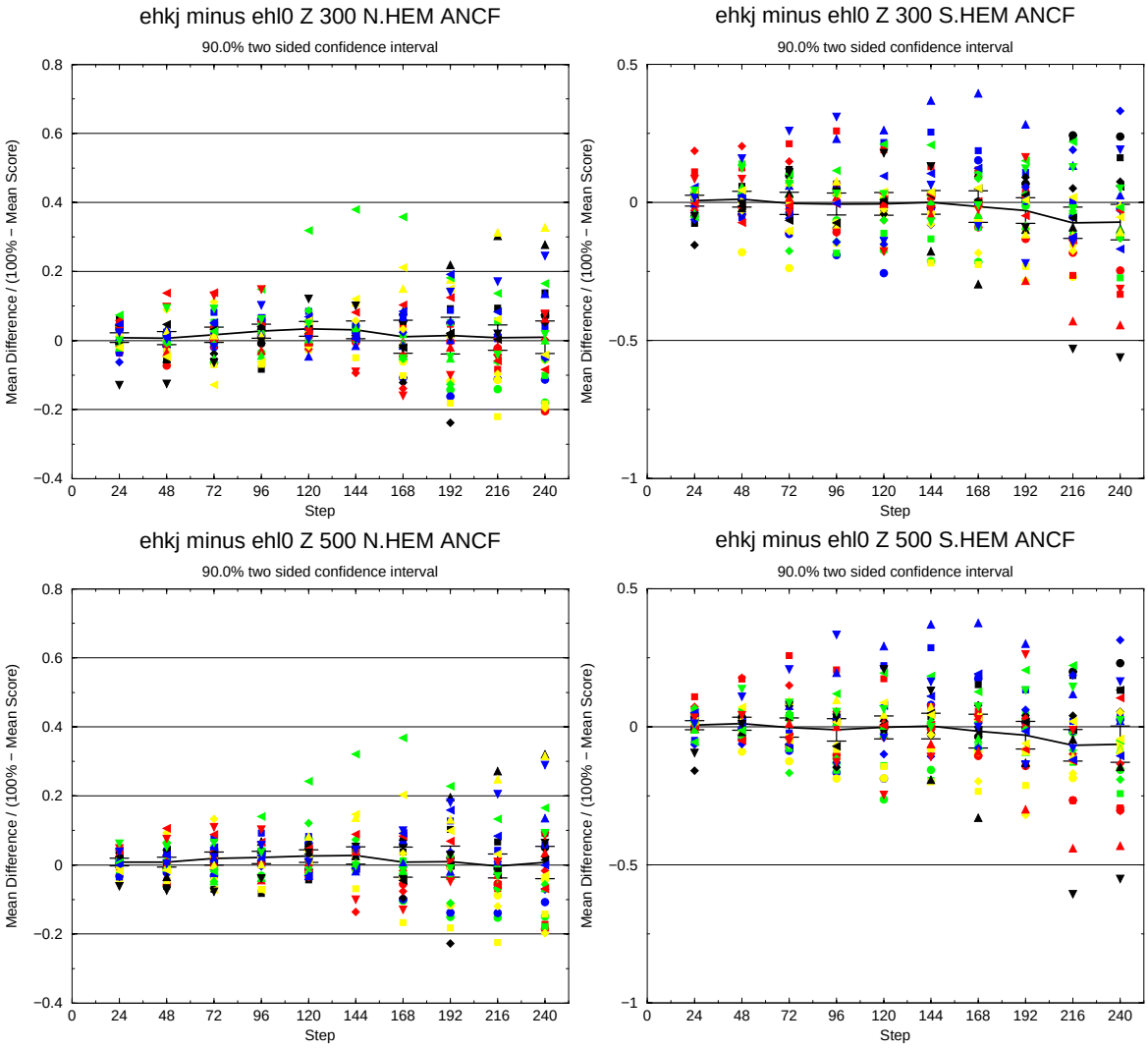

Figure 28: Difference between Meteosat-8 assimilation with $\mathbf{R} = diag(4.0, 4.0)$ K^2 and control anomaly correlation of height field forecasts. 300 hPa fields are shown above, 500 hPa below, northern hemisphere on the left and southern hemisphere on the right. Line marks mean difference and error bar marks 90% confidence region adjusted for one step autocorrelation.

Meteorol. Soc., **127**, 1453-1468

Köpken, C., Kelly G. and Thépaut, J.-N., 2004: Assimilation of Meteosat radiance data within the 4D-Var system at ECMWF: Assimilation experiments and forecast impact, *Q. J. R. Meteorol. Soc.*, in press.

Lutz, H.-J., 1999: Cloud processing for Meteosat Second Generation. *Technical Memorandum No. 4* Available from EUMETSAT, Am Kavallerisand 31, 64295 Darmstadt, Germany.

Schmetz, J., Pili, P. and Tjemkes, S. 2000: Meteosat Second Generation (MSG) Pp. 111-121 in proceedings of ECMWF seminar on exploitation of the new generation of satellite instruments for numerical weather prediction, 4-8 September 2000, ECMWF, Reading, UK

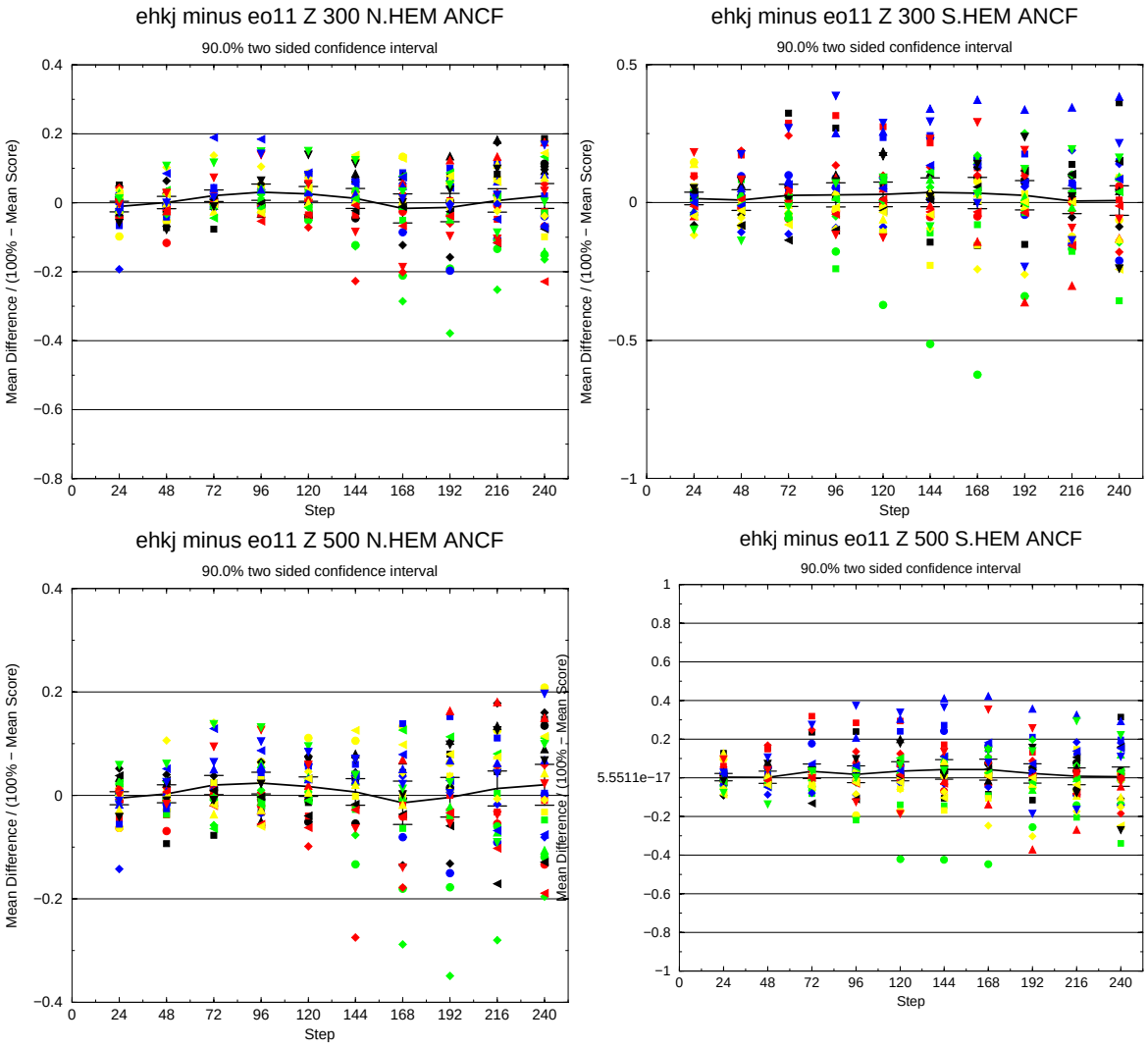

Figure 29: Difference between Meteosat-8 assimilation with $\mathbf{R} = diag(4.0, 4.0)$ K^2 and operations (i.e. including Meteosat-7 assimilation) anomaly correlation of height field forecasts. 300 hPa fields are shown above, 500 hPa below, northern hemisphere on the left and southern hemisphere on the right. Line marks mean difference and error bar marks 90% confidence region adjusted for one step autocorrelation.

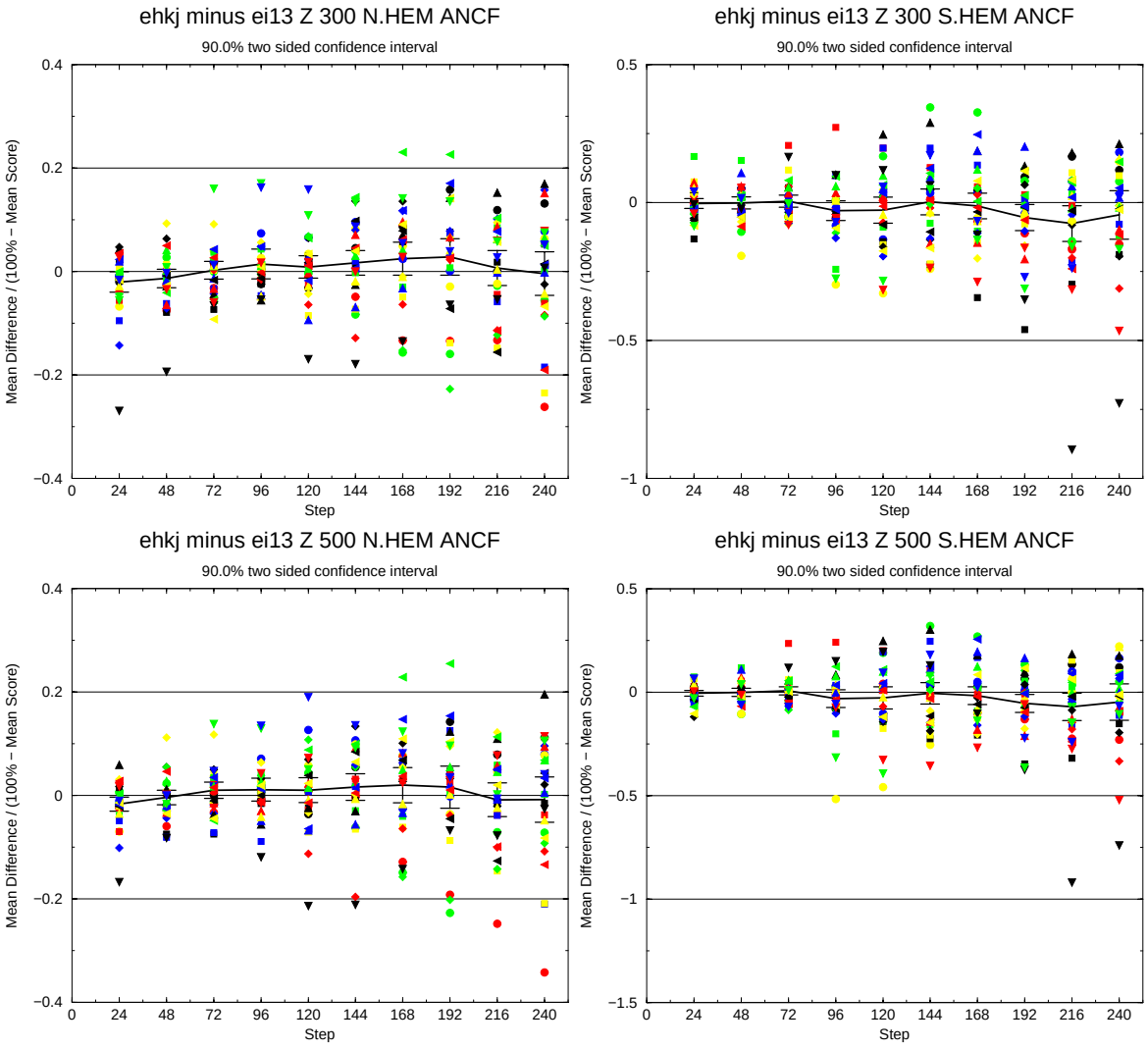

Figure 30: Difference between Meteosat-8 assimilation with $\mathbf{R} = diag(4.0, 4.0)$ K^2 and Meteosat-8 assimilation with $\mathbf{R} = diag(4.0, 2.25)$ K^2 anomaly correlation of height field forecasts. 300 hPa fields are shown above, 500 hPa below, northern hemisphere on the left and southern hemisphere on the right. Line marks mean difference and error bar marks 90% confidence region adjusted for one step autocorrelation.

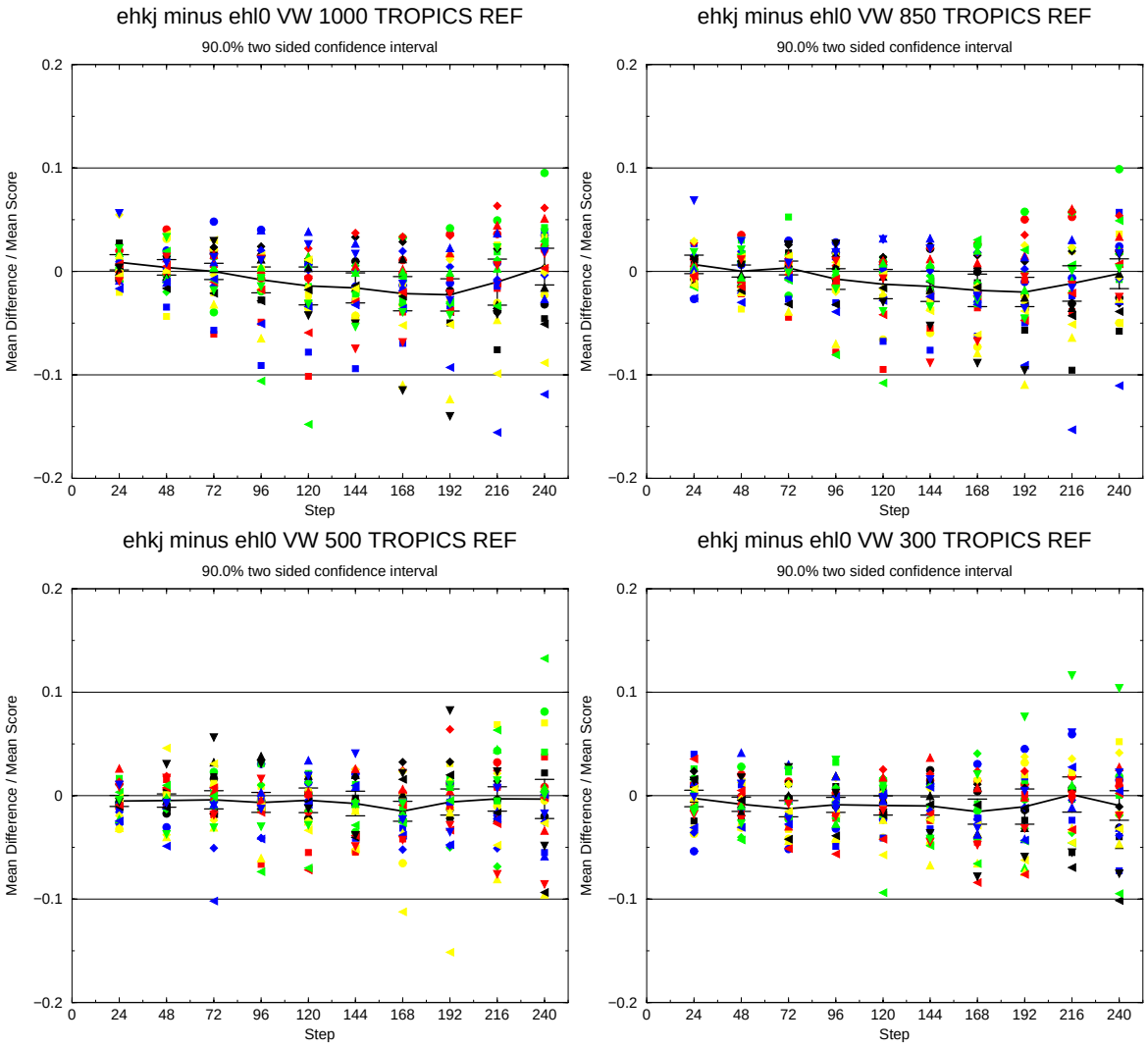

Figure 31: Difference between Meteosat-8 assimilation with $\mathbf{R} = diag(4.0, 4.0)$ K^2 and control RMS error in tropical vector wind field forecasts at 1000, 850, 500 and 300 hPa. Line marks mean difference and error bar marks 90% confidence region adjusted for one step autocorrelation.